Trisubstituted Acridine Derivatives as Potent and Selective Telomerase Inhibitors

R. John Harrison,[†] Javier Cuesta,[†] Gianni Chessari,[†] Martin A. Read,[†] Sanji K. Basra,[†] Anthony P. Reszka,[†] James Morrell,[†] Sharon M. Gowan,[‡] Christopher M. Incles,[†] Farial A. Tanious,[§] W. David Wilson,[§] Lloyd R. Kelland,[‡,#] and Stephen Neidle*[,†]

Cancer Research UK Biomolecular Structure Group, The School of Pharmacy, University of London, 29-39 Brunswick Square, London, WC1N 1AX, U.K., Cancer Research UK Centre for Cancer Therapeutics, Sutton, Surrey SM2 5NG, U.K., and Department of Chemistry, Georgia State University, Atlanta, Georgia 30303-3083

Received April 9, 2003

The synthesis and evaluation for telomerase-inhibitory and quadruplex DNA binding properties of three related series of rationally designed trisubstituted acridine derivatives are described. These are substituted on the acridine ring at the 2,6,9; 2,7,9; and 3,6,9 positions. The ability of several of the most potent compounds to interact with and stabilize an intramolecular G-quadruplex DNA was evaluated by surface plasmon resonance methods, and affinities were found to correlate with potency in a telomerase assay. The interactions of a number of compounds with a parallel quadruplex DNA structure were simulated by molecular modeling methods. The calculated interaction energies were compared with telomerase activity and showed generally consistent correlations between quadruplex affinity and telomerase inhibition. These data support a model for the action of these compounds that involves the stabilization of intermediate quadruplex structures that inhibit the elongation of telomeric DNA by telomerase in tumor cells.

Introduction

The ends of chromosomes comprise guanine-rich tandem-repeating DNA sequences,[1] typically 6−12 kb in length in humans, that are associated with a number of structural and regulatory proteins.[2] A key function of telomeres is to protect chromosome ends from base-pair loss and end-to-end fusions, thereby safeguarding the integrity of each chromosome. Telomere erosion occurs naturally during replication of somatic cells, with ca. 50−200 base pairs lost per round of division as a result of the inability of DNA polymerase to fully replicate the ends[3]—the "end-replication problem". These cells continue to function and divide until a critically short length of telomeric DNA is reached, when cells enter a stage of irreversible growth arrest, replicative senescence,[4] followed by cell crisis and apoptosis. Tumor cells are notable exceptions to this behavior, both in primary tumors and tumor cell lines, where the DNAs of their telomeres are maintained in length so that they are effectively immortalized.[5] This maintenance of tumor telomeric DNA is achieved in 80−85% of these cells by the activation of the specialized reverse transcriptase enzyme complex telomerase, which elongates telomeres by catalyzing the addition of further tandem repeat sequences.[6] Telomerase expression is necessary for the maintenance of immortalized cancer cells and for their proliferation of cancer cells.[7] Those cell lines that do not express telomerase maintain telomere length by the ALT (alternative) pathway, which involves recombination processes.[8] Telomeric DNA in tumor cells has a range of lengths whose average, depending on cell type, is significantly shorter than those in somatic cells, with 3−6 kb being typical. ALT cell lines such as the osteosarcoma line GM847 tend to have significantly longer telomeres, 9−12 kb, in a similar range as telomeres in normal human somatic cells.

Proof of principle that telomerase inhibition can lead to selective anticancer effects in tumor cells has been demonstrated using dominant-negative mutants of the catalytic domain of telomerase (hTERT),[9] with telomere shortening and senescence being observed. Similar effects have been found with hTERT catalytic-site inhibitors[10] and antisense molecules directed against hTR.[11] The classic model for inhibition of telomere maintenance and telomerase activity as a potential anticancer therapy[12] suggests that the inhibition of telomerase in tumor cells will initially result in telomere shortening at each successive round of replication. This will eventually drive telomerase-positive tumor cells to senescence prior to normal (and germ line) cells as a consequence of the significantly shorter length of telomeric DNA in the former cells. Thus, any selective anticancer therapeutic response involving senescence and apoptosis of cancer cells would only occur after they had undergone a large number of rounds of replication. This long-term treatment would also necessitate minimal toxicity for the agents being used, with high ^{tel}TI values (where the therapeutic index ^{tel}TI is defined as the ratio of telomerase inhibitory ability $^{tel}EC_{50}$ to acute cellular toxicity, IC_{50}).

There are a number of strategies that have been reported for telomerase inhibition, including inhibition of the catalytic active site of the enzyme[10] and antisense oligonucleotide competition with the 3′ end of telomeric

* To whom correspondence should be addressed. Phone: 44 207 753 5969. Fax: 44 207 753 5970. E-mail: stephen.neidle@ulsop.ac.uk.
[†] University of London.
[‡] Cancer Research UK Centre for Cancer Therapeutics.
[§] Georgia State University.
[#] Present address: Antisoma Research Laboratories, St. George's Hospital Medical School, Cramner Terrace, London SW17 0QS, U.K.

10.1021/jm0308693 CCC: $25.00 © 2003 American Chemical Society
Published on Web 09/06/2003

DNA for the template site on the RNA subunit (hTR) of telomerase.[11] Both these approaches have been shown to result in telomere shortening, and for the former at least, in vivo antitumor effects have been observed, albeit only after extended time scales have elapsed. An alternative approach[12,13] involves the stabilization of higher-order quadruplex structures formed by the guanine-rich telomeric DNA primer, which is single-stranded for the terminal 100−200 bases at the extreme 3′ end of telomeric DNA in human chromosomes.[14] This is based on the requirement to maintain this single-strandedness when the terminal bases are recognized by the complementary sequence of the RNA template of telomerase, the essential first step prior to the synthesis by hTERT of further telomeric DNA repeats. It has been earlier demonstrated that induction of telomere folding to form four-stranded quadruplex structures containing the characteristic quartets of hydrogen-bonded guanines[15] results in inhibition of telomerase activity.[16]

We have previously reported that compounds based on planar tricyclic chromophore frameworks consisting of anthraquinones,[17] fluorenones,[18] or acridines,[19] disubstituted with appropriate aminoalkylamido groups, can both stabilize G-quadruplex structures and inhibit telomerase activity in vitro. The primary requirement is for a central planar pharmacophore capable of binding to guanine tetrads by means of $\pi-\pi$ interactions. At least two side chains of minimal length ($-NHCOCH_2-CH_2-$) are also required, which molecular modeling studies have suggested[19b] are directed toward the quadruplex grooves. Tertiary amine functionality is required at the terminii of the side chains. These amines are required to be protonated at physiological pH. The size of the amine substituents is also important, with bulky amines disrupting quadruplex binding and reducing potency of enzyme inhibition.[19b]

A number of other G-quadruplex-binding ligands have been reported, notably based on substituted porphyrins,[20] various substituted polycyclic compounds,[21] phenanthroline and triazine derivatives,[22] and quinolines.[23] The natural product telomestatin, comprising one thiazoline and seven oxazole rings in a cyclic arrangement, has been reported to be a potent nanomolar inhibitor of telomerase,[24] with evidence indicating that its mechanism of action also involves the formation of a G-quadruplex complex.[25]

Ligands based on the acridine skeleton have been subsequently developed by us as starting points for ligands with enhanced selectivity for quadruplex binding and telomerase potency on account of their synthetic accessibility, as well as the established druglike properties of many acridine-based compounds.[26] We have previously used rational structure-based design methods, leading to derivatization at the 9-position of the 3,6-disubstituted acridine ring system.[27] The initial trisubstituted compounds that were reported (compounds **7** and **8** here) showed a marked improvement in selectivity for telomerase inhibition and G-quadruplex affinity over disubstituted ones, with the $^{tel}EC_{50}$ value for the optimal 3,6,9-trisubstituted compound being 0.06 μM compared to ca. 1−5 μM for the optimal compounds in the 3,6-disubstituted series.[19] Subsequent studies have shown that one of these trisubstituted compounds produces growth arrest and senescence in long-term cell assays and shows in vivo antitumor activity.[28]

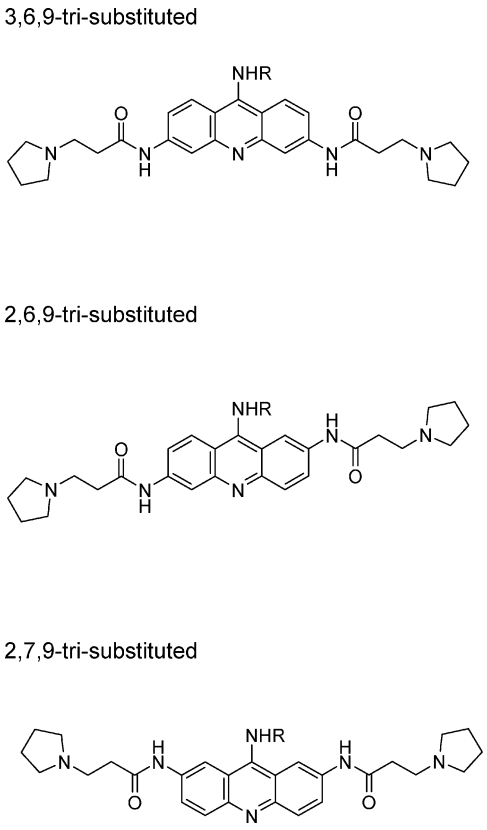

Figure 1. Trisubstituted acridine regioisomers.

We report here a systematic study of a range of substituents at the 9-position in 3,6,9-trisubstituted acridines, as well as the regioisomeric 2,6,9 and 2,7,9 acridines (Figure 1). Molecular modeling studies have been used in order to rationalize their telomerase-inhibitory activity and relate it to quadruplex-binding behavior. The crystal structure of the human intramolecular 22-mer quadruplex[29] has been employed as the starting point in these modeling studies rather than the NMR structure[30] used in earlier work, since the former was determined in the presence of physiological levels of potassium ions whereas the latter was analyzed in the presence of sodium ions.

Results

Chemistry. We have previously described[19] syntheses of several of the acridone starting materials **1**−**3**. The key 9-chloroacridine intermediates **4**−**6** were prepared in each series by treatment of the acridone precursor with excess $POCl_3$ and refluxing for 3 h. Filtration and base wash provided the desired compounds in high yield. The route to the trisubstituted compounds involves substitution of 9-chloroacridines, which has been described in the literature to take place under a variety of conditions including use of phenol, methanol, and copper. However, it was found for the preparation of the compounds described here that direct treatment of the 9-chloro intermediate with a suitable amine by refluxing in chloroform provided the desired compounds in high yield (Scheme 1). The hydrochloride salt of each derivative was prepared to improve water solubility, for biological and biophysical evaluation. In

Scheme 1. Synthesis of Trisubstituted Acridine Derivatives[a]

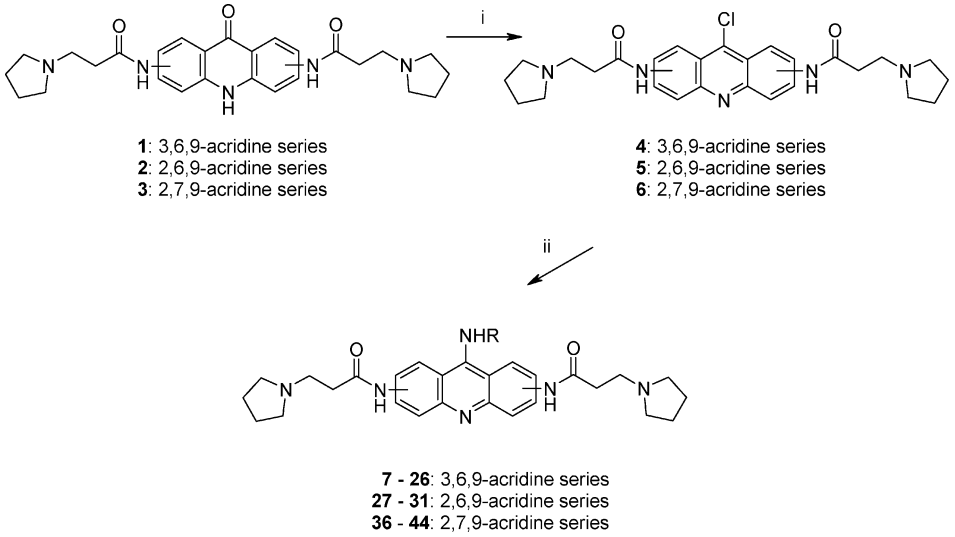

[a] (i) $POCl_3$, reflux; (ii) H_2N-R, $CHCl_3$.

every case, the identical side chains at the 2,6-, 2,7-, or 3,6-position were employed, all terminating in a pyrrolidino ring. Previous studies of the 3,6-series[19] had shown that this was an optimal choice, at least for the side chains explored to date.

Biological Activity and Structure−Activity Relationships. All compounds were evaluated for their effects in vitro on short-term inhibition of cell growth against a panel of two human epithelial carcinoma cell lines, using the sulforhodamine B (SRB) assay.[31] Results are presented in Table 1 as the concentrations required to inhibit cell growth by 50% (IC_{50} values). All compounds were tested for their ability to inhibit Taq polymerase prior to their evaluation in a PCR-based telomerase assay. Compounds were tested at concentrations of 1.0, 10, 20, and 50 μM. Those that did not inhibit Taq at these concentrations were subsequently evaluated for their ability to inhibit human telomerase in a modified cell-free TRAP (telomerase repeat amplification protocol) assay using extracts from the A2780 cell line.[17−19] Agents were tested at concentrations of 0.1, 0.5, 1, 5, 10, 20, and 50 μM up to the concentration that Taq polymerase inhibition was first observed. The concentrations required to inhibit telomerase activity by 50% ($^{tel}EC_{50}$ values) are also reported in Table 1.

Almost all of the trisubstituted acridine compounds reported here have $^{tel}EC_{50}$ values that are less than 1 μM, with the exception of one compound in the 2,6,9-series and four in the 2,7,9-series. All compounds in the 3,6,9-series have values less than 0.2 μM, which is generally the most potent of the three regioisomer groups (Table 1), even though not all members of these series were accessible because of difficulties in obtaining sufficient analytically pure material in every instance. The trends are illustrated in Figure 2a. The 2,7,9-series is the least potent overall. These differences may be clearly seen by comparing equivalent compounds in the three series, for example, those with $NHPh-NR_2$ substituents. Thus, compounds **7** and **8** have telomerase potencies of 115 and 74 nM, respectively, their analogues in the 2,6,9-series (compounds **26** and **27**) have potencies of 80 and 170 nM, and the two in the 2,7,9-series (compounds **38** and **39**) have potencies of 200 and 500 nM. The ortho, meta, and para isomers of the phenyl-NH_2 and phenyl-NMe_2 derivatives also show differences in their behavior, although the pattern is more complex, with trends being restricted to a particular series. Thus, in the 3,6,9-series, the *o*-NH_2 phenyl derivative **12** is approximately 3-fold more active than its meta and para counterparts **8** and **11**. Differences in the slightly less-active 2,6,9-series between these three isomers are less marked, whereas they are more accentuated in the 2,7,9-series.

In general, the results show clearly that the anilino substituent at the 9-position is not an absolute requirement for activity, and compounds with a simple acyclic or cyclic side chain at this position can show comparable activity (for example, compound **19**). The size of the 9-substituent is a factor in telomerase inhibition, with short aliphatic chains of four to five atoms imparting the greatest activity in all three series. This has been most explored in the 3,6,9-series, with those compounds having a cationic end-group, such as **9**, **18**, and **19**, showing optimal activity. The last two, with $^{tel}EC_{50}$ values of 18 nM, are the most potent reported here and are among the most potent telomerase inhibitors of any type found to date. It is also notable that those derivatives with nonbasic or even hydrophobic side chains, typified by compounds **17** and **14**, **16** and **22**, still retain good activity, although this appears to decrease with increasing side chain length or size of ring (cf. the slightly reduced activity of compound **16** compared to **14** and **22**).

None of the compounds reported here have acute toxicities (IC_{50} values) in ranges comparable to $^{tel}EC_{50}$ values, although considerable differences in behavior are apparent. In general, enhanced potency for telomerase inhibition is paralleled by weaker acute toxicity (see, for example, compounds **7**, **8** vs **18**, **19**). There is a clear correlation between the number of ring carbon atoms and toxicity for compounds such as **14**, **16**, and **22**, suggesting that increased hydrophobicity contributes to higher IC_{50} values Those compounds with (relatively) longer side chains terminating in a basic nitrogen atom, such as **9**, **10**, **18**, and **19**, have optimal $^{tel}EC_{50}/IC_{50}$ ratios.

Table 1. Telomerase Inhibition and Acute Cellular Toxicity Data for the Trisubstituted Compounds[a]

Compound Number	9-substituent	Isomer	$^{tel}EC_{50}$, μM	esd	Cytotoxicity IC_{50}, μM A2780	A431
44	-	3,6	5.2	0.3	2.6	-
7	NHPh-para-NMe_2	3,6,9	0.115	0.025	10	15.8
8	NHPh-para-NH_2	3,6,9	0.074	0.014	25	25
11	NHPh-meta-NH_2	3,6,9	0.06	0.02	12.6	12.6
12	NHPh-ortho-NH_2	3,6,9	0.02	0.004	11	7.1
13	NHPh-meta-NMe_2	3,6,9	0.1	0.04	7.9	2
17	NHPh-para-$COCH_3$	3,6,9	0.04	0.02	3.2	2.2
21	NHPh-meta-$NHCOCH_3$	3,6,9	0.1	0.02	>25	>25
23	NHPh-para-F	3,6,9	0.07	0.02	3.2	0.5
24	NHPh-ortho-SMe	3,6,9	0.15	0.03	0.1	2.5
25	NHPh-meta-SMe	3,6,9	0.1	0.06	2.8	1.3
26	NHPh-para-NH_2	2,6,9	0.08	0.002	>25	>25
27	NHPh-para-NMe_2	2,6,9	0.17	0.021	7.9	10
29	NHPh-meta-NH_2	2,6,9	0.21	0.028	15.8	>25
30	NHPh-ortho-NH_2	2,6,9	0.11	0.021	15.8	>25
31	NHPh	2,6,9	1.33	0.155	5.6	14
34	NHPh-para-OMe	2,7,9	0.46	0.185	10	12.6
35	NHPh-ortho-NH_2	2,7,9	0.17	0.01	17.8	>25
36	NHPh-meta-NH_2	2,7,9	1.09	0.41	6.3	>25
37	NHPh-meta-NMe_2	2,7,9	0.6	0.29	3.2	12.6
38	NHPh-para-NH_2	2,7,9	0.2	0.025	>25	>25
39	NHPh-paraNMe_2	2,7,9	0.5	0.301	19	>25
40	NHPh	2,7,9	1.29	0.3	2.6	12.5
41	NHPh-meta-OMe	2,7,9	2.73	0.317	2.5	10
42	NHPh-ortho-OH	2,7,9	1.03	0.201	10	>25
9	$NHCH_2CH_2CH_2NMe_2$	3,6,9	0.06	0.001	>25	>25
10	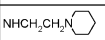	3,6,9	0.05	0.008	12.6	11.2
14	NHC_6H_{11}	3,6,9	0.09	0.02	12.5	2.5
15	$NHCH_2CH_2OMe$	3,6,9	0.14	0.004	10	10
16	NHC_7H_{13}	3,6,9	0.21	0.02	3.2	3.2
18	$NHCH_2CH_2NMe_2$	3,6,9	0.018	0.002	>25	>25
19		3,6,9	0.018	0.003	>25	25
20	$NHCH_2$-meta-Pyridine	3,6,9	0.066	0.01	>25	>25
22	NHC_3H_5	3,6,9	0.05	0.05	19	>25
28	$NHCH_2CH_2NMe_2$	2,6,9	0.27	0.046	>25	>25
32	$NHCH_2CH_2CH_2NMe_2$	2,6,9	0.08	0.024	>25	>25
33	NHC_6H_{11}	2,6,9	0.21	0.008	10	14
43	$NHCH_2CH_2NMe_2$	2,7,9	0.57	0.014	11	>25

[a] Compounds are listed in order of whether the 9-substituents are aromatic or aliphatic. Compound **44** is the 3,6-disubstituted acridine with a pyrrolidino group at the terminus of each side chain.

Binding to DNAs. Table 2 gives affinity constants for four representative trisubstituted compounds binding to the human 22-mer quadruplex structure and to a representative G-rich duplex DNA sequence, compared to the disubstituted analogue.[19] All of the acridine compounds have a single strong binding site on the quadruplex and typically have a weaker secondary binding interaction with 10- to 20-fold lower affinity. All four of the trisubstituted acridines bind with significantly greater (at least 10-fold) affinities to the quadruplex, with compound **19** having around a 100-fold greater affinity than compound **44**, one of the best in the earlier disubstituted series. There is an overall clear trend of quadruplex affinity relating to telomerase inhibitory potency, despite the small number of compounds examined, comparing **9**, **10** with **18**, **19**.

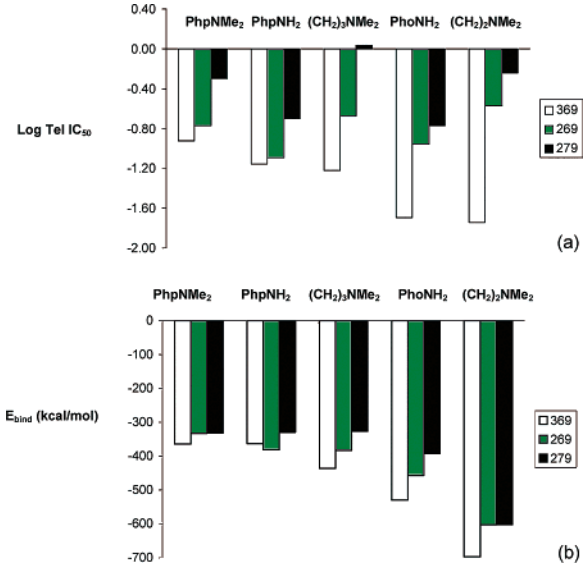

Figure 2. Histograms of (a) telomerase activity as $^{tel}EC_{50}$ values and (b) computed interaction energies in kcal mol^{-1} for selected compounds, grouped according to substituent and substitution pattern.

Table 2. Affinity Constants (M^{-1}) for Selected Acridine Derivatives Binding to Duplex and Quadruplex DNA Structures (See Text)[a]

compd	duplex	quadruplex
7	4×10^5	1.6×10^7
8	5×10^5	1.6×10^7
18	4.9×10^6	5.7×10^7
44	1.1×10^6	1.3×10^6

[a] Values were obtained from surface plasmon resonance analysis. Compound **44** is the 3,6-disubstituted acridine with a pyrrolidino group at the terminus of each side chain.

The trisubstituted compounds all show reduced duplex affinity compared to their quadruplex binding. Compounds **18** and **19** both have slightly elevated duplex affinities compared to **7** and **8**, although this is not reflected in their patterns of IC_{50} values. Both the association and dissociation kinetic constants are lower for binding of the acridines to quadruplex relative to the duplex. The effect on the dissociation constant is greater, and this results in the greater observed affinity constant of the acridines for the quadruplex.

Molecular Modeling. We have adopted a simple molecular modeling approach, as described in the Experimental Section, to compare the measurements of telomerase inhibition ($^{tel}EC_{50}$ values) with the intermolecular interactions between the intramolecular telomeric DNA G-quadruplex and the trisubstituted acridines reported here. The relative binding energies (E_{bind}) of each complex have been calculated considering only van der Waals and the Coulombic contributions. In this way, we have been able to assess a large number of compounds on a realistic time scale. These energies are not equivalent to the experimental free energy of binding because different aspects of the binding process such as solvation effects, entropic contribution, and cooperativity have not been taken into account. Instead, we consider these contributions to be broadly similar for all the compounds because all the 9-substituents are

Table 3. Calculated Interaction Energies (in kcal mol^{-1}) for the Trisubstituted Compounds Bound to the 22-mer G-Quadruplex

			Calculated energy		
Compound	NHR	pattern	E_{vdW}	E_{Coul}	E_{bind}
7	$NHPhpNMe_2$	3,6,9	-42.68	-321.75	-364.43
8	$NHPhpNH_2$	3,6,9	-41.44	-321.70	-363.14
9	$NHCH_2CH_2CH_2NMe_2$	3,6,9	-49.45	-659.55	-709.00
11	$NHPhmNH_2$	3,6,9	-42.44	-394.12	-436.56
12	$NHPhoNH_2$	3,6,9	-45.30	-484.46	-529.76
13	$NHPhmNMe_2$	3,6,9	-42.57	-257.91	-300.47
17	$NHPhpCOCH_3$	3,6,9	-43.92	-391.11	-435.03
21	$NHPhmNHCOCH_3$	3,6,9	-42.43	-261.51	-303.94
23	NHPhpF	3,6,9	-41.45	-323.45	-364.91
24	NHPhoSMe	3,6,9	-42.58	-260.17	-302.75
25	NHPhmSMe	3,6,9	-41.83	-260.17	-302.00
26	$NHPhpNH_2$	2,6,9	-48.10	-333.66	-381.76
27	$NHPhpNMe_2$	2,6,9	-45.75	-287.44	-333.19
29	$NHPhmNH_2$	2,6,9	-48.01	-335.15	-383.16
30	$NHPhoNH_2$	2,6,9	-48.00	-409.18	-457.18
35	$NHPhoNH_2$	2,7,9	-45.73	-346.6	-392.33
36	$NHPhmNH_2$	2,7,9	-40.96	-285.81	-326.77
38	$NHPhpNH_2$	2,7,9	-41.29	-288.58	-329.87
39	$NHPhpNMe_2$	2,7,9	-43.11	-288.98	-332.09
10	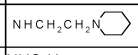	3,6,9	-48.39	-538.93	-587.32
14	NHC_6H_{11}	3,6,9	-46.99	-393.21	-440.20
15	$NHCH_2CH_2OMe$	3,6,9	-44.21	-394.09	-438.30
16	NHC_7H_{13}	3,6,9	-48.01	-394.06	-442.07
18	$NHCH_2CH_2NMe_2$	3,6,9	-47.20	-650.52	-697.72
20	$NHCH_2$mPyridine	3,6,9	-47.68	-548.03	-595.71
22	NHC_3H_5	3,6,9	-43.50	-481.10	-524.60
28	$NHCH_2CH_2NMe_2$	2,6,9	-49.59	-553.77	-603.36
43	$NHCH_2CH_2NMe_2$	2,7,9	-48.99	-553.59	-602.58

occupying a broadly similar volume in a groove of the quadruplex structure. In this way, we have been able to rapidly calculate E_{bind} values for 28 compounds. These values are given in Table 3 and compared in Figures 2 and 3 to rank the acridine compounds in terms of the best interacting compounds with telomeric DNA and to compare these results with the biological in vitro data.

The 22-mer X-ray crystal structure[29] of d[AGGG-(TTAGGG)$_3$] is characterized by two external G-quartet planes, which can be used as docking binding sites for the acridine derivatives. As a first step, it was necessary to determine which of these two surfaces is optimal for ligand binding. The 5′ G-quartet surface is hydrophobic, whereas the 3′ G-quartet one is more hydrophilic. The trisubstituted acridines can interact with both G-quartet faces through the formation of a strong electrostatic interaction between the positively charged acridinium nitrogen and the highly electron-rich central area of the G-quartet plane due to the guanine carbonyl lone pairs. The 5′ G-quartet surface would be expected to be favored for $\pi-\pi$ aromatic stacking interactions between the acridine scaffold and the G-quartet plane on account of its greater hydrophobicity compared to the 3′ one. Finally, the three side chains lie in three different grooves, conferring selectivity toward the G-quadruplex DNA structure to the acridine scaffold. However, when the more hydrophilic 3′ G-quartet plane was used as the binding site, it was observed that the side chains of the trisubstituted acridines interacted better with the particular TTA loop conformation present in the 22-mer

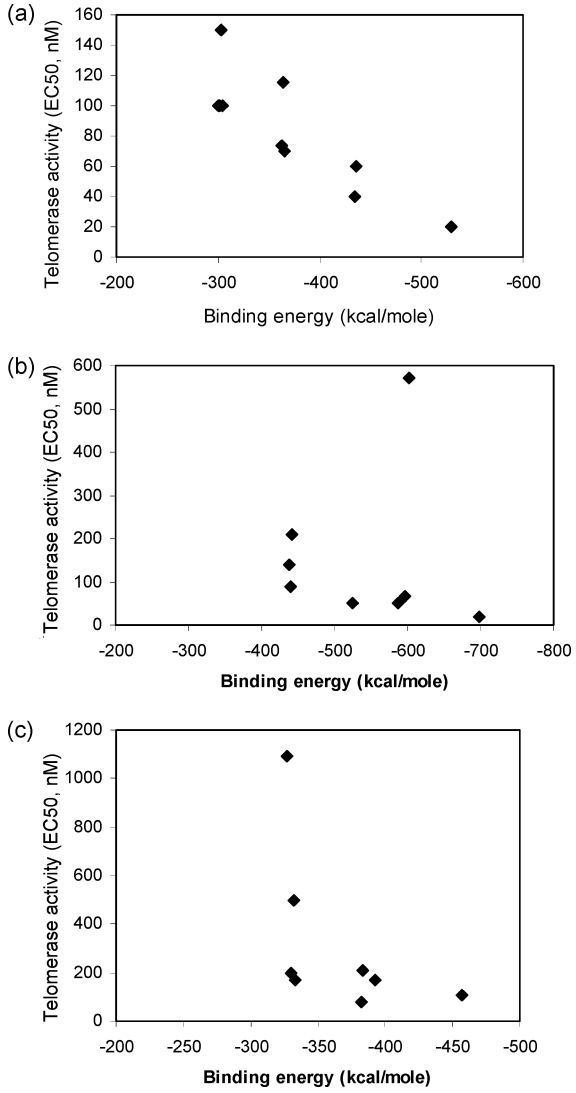

Figure 3. Plots of calculated binding energies, from Table 3, vs telomerase inhibition, shown as EC_{50} values, for three subsets of ligands: (a) for **7**−**25**, with 3,6,9-substitution and an aniline group at the 9-position; (b) for **10**−**43**, with an aliphatic group in the 9-position; (c) for **26**−**39**, with 2,6,9- and 2,7,9-trisubstitution and an anilino group at the 9-position.

X-ray crystal structure, resulting in lower E_{bind} values. Therefore, the 3′ G-quartet face was used as the binding site for the docking of all the acridine compounds. The prediction of a single strong binding site and a significantly weaker secondary site is supported by the surface plasmon resonance results described above.

Position 9 of the three different regioisomer scaffolds (2,6,9; 2,7,9; 3,6,9) has been extensively functionalized in this study with different aliphatic and aromatic side chains. Figure 4a−e shows the results from the modeling studies of a representative active compound (**18**, **28**, **43**) in each of the three different patterns, binding to the 22-mer structure. In each case the group in the 9-position points directly into a DNA groove, as does the anilino group in compounds such as **11** (Figure 4f). The particular conformation adopted by the side chains in the 3,6,9-scaffold brings the 9-position substituents significantly deeper into the cavity of this groove when compared to the other scaffold families. Therefore, functionalities attached to the 9-position in the 3,6,9 acridine scaffold can interact better with the surface of

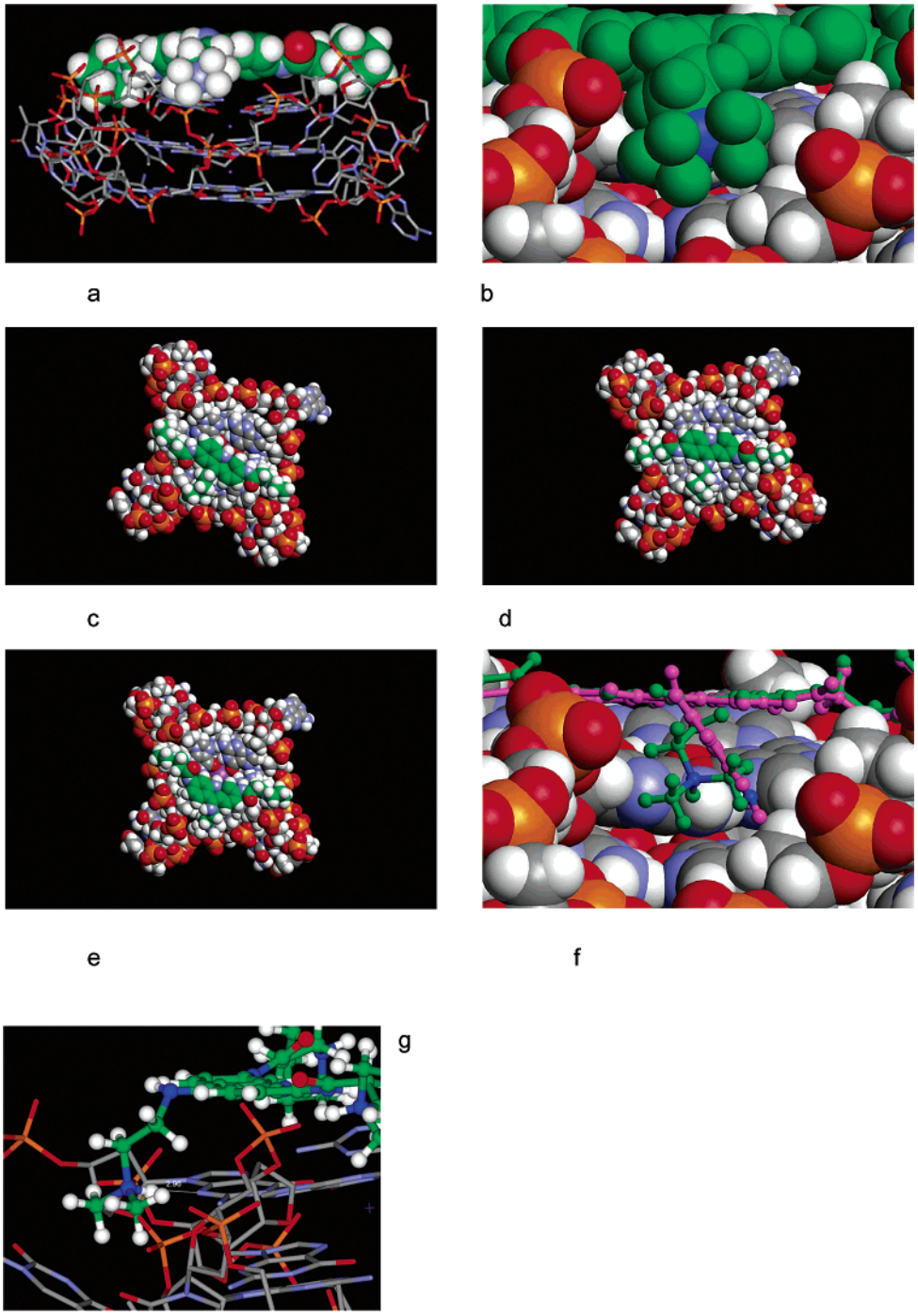

Figure 4. Plots from molecular modeling studies showing various ligands interacting with the human 22-mer intramolecular quadruplex: (a) side view of compound **18** (in van der Waals representation) and the quadruplex in stick form; (b) enlarged van der Waals surface representation of the computed complex with the 3,6,9-trisubstituted compound **18**, showing the quadruplex groove with the 9-substituent $NH(CH_2)_2N^+HMe_2$; (c) view onto the plane of the G-quartets of the modeled complex with the 2,6,9-trisubstituted compound **28** with the 9-substituent $NH(CH_2)_2N^+HMe_2$; (d) view onto the plane of the G-quartets of the modeled complex with the 2,7,9-trisubstituted compound **43** with the 9-substituent $NH(CH_2)_2N^+HMe_2$; (e) view onto the plane of the G-quartets of the modeled complex with the 3,6,9-trisubstituted compound **18** with the 9-substituent $NH(CH_2)_2N^+HMe_2$; (f) view looking into the groove, showing the overlay of compounds **11** (in mauve) and **18** (in green), emphasizing the similar region occupied by their 9-substituents, where the nitrogen atoms of the ligands are blue; (g) view of the quadruplex complex with compound **18**, showing the potential hydrogen-bond interaction with a guanine N3 atom.

this groove without creating steric clashes, especially when they carry a positive charge, as in the case of the 9-substituent terminal protonated nitrogen atom in compound **18** (Figure 4g).

The 3,6,9 acridines have overall the highest calculated binding energies (lower E_{bind} values) to the human G-quadruplex structure, compared with the corresponding 2,6,9 and 2,7,9 regioisomers (see also Figure 2b). Table 3 gives the calculated E_{bind} values for the complexes between the 22-mer and members of the three series of acridine compounds. The pattern of energies compares well overall with the experimental telomerase $^{tel}EC_{50}$ values in Figure 2a (see below). All compounds have approximately constant van der Waals contribu-

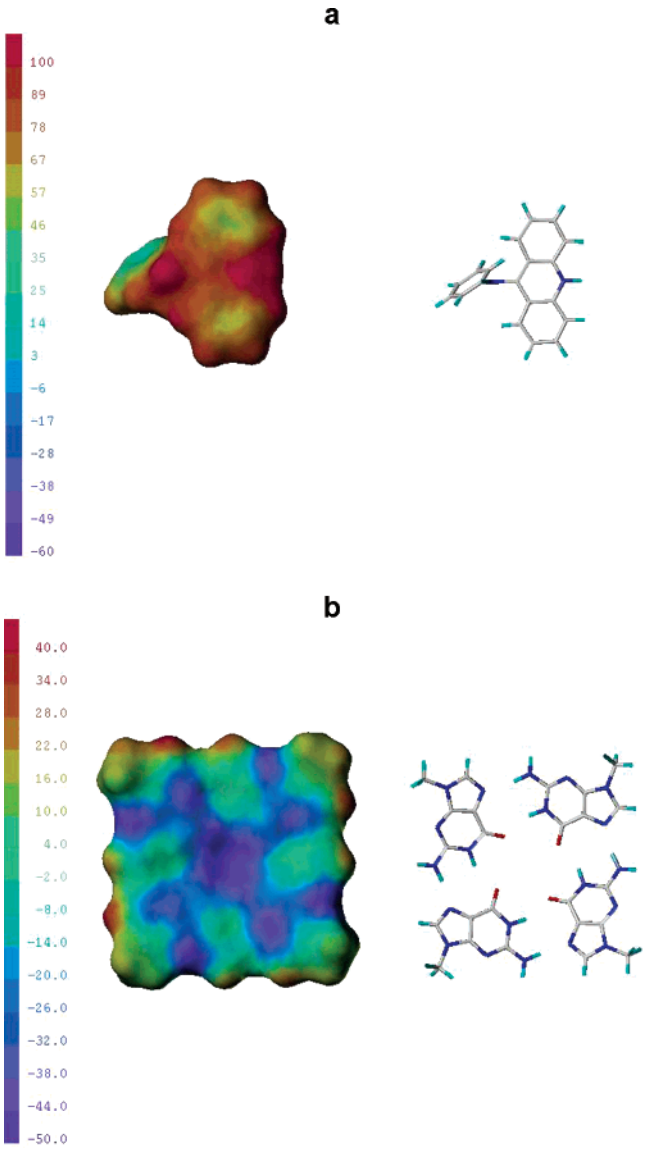

Figure 5. Calculated semiempirical partial charges represented by Connolly surfaces colored by charge distribution (a) for 9-phenylacridine and (b) for a guanine quartet. In part a, the region of positive electrostatic potential around the protonated ring nitrogen atom is clearly visible. In part b, the extended region of negative electrostatic potential in the central region, arising from the presence of the four O6 atoms, is highlighted in blue.

tions to the total energy, suggesting that the electrostatic contribution is the driving force for the binding of the compounds with greatest affinity and potency. This trend is especially apparent for the acyclic compound **18**, which carries a formal positive charge at their terminus and is one of the best compounds overall in the series in terms of telomerase inhibitory activity. The space occupied by the side chain of this compound compares well with that for the phenyl substituents such as compound **11** (see Figure 4f), but crucially the protonated nitrogen atom in **18** can form a hydrogen bond having excellent geometry (Figure 4g) with a quadruplex guanine N3 atom (the donor···acceptor distance is 3.0 Å). The superior calculated binding energy of **18** compared to that of **11** is in accord with their relative $^{tel}EC_{50}$ values (Table 1). Compound **9**, with a one-carbon longer side chain, makes slightly superior

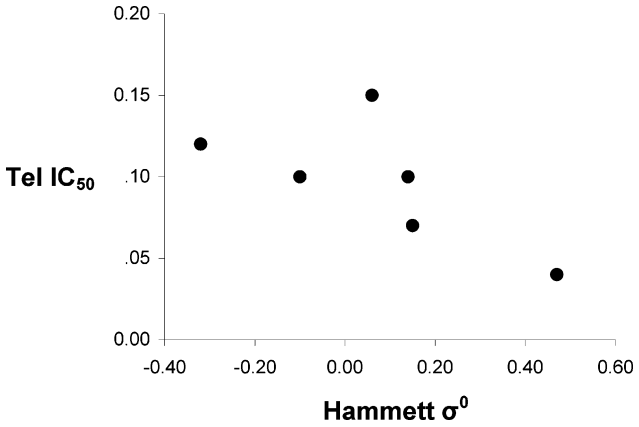

Figure 6. Plot of calculated Hammett σ values for a set of 3,6,9-trisubstituted anilino derivatives (compounds **7**, **13**, **18**, **24**−**26**) vs telomerase activity ($^{tel}EC_{50}$, in μM).

electrostatic and van der Waals interactions with the groove cavity compared to compound **18**. However, **9** is about 3-fold less active against telomerase, suggesting that the modeling approach adopted here cannot always be relied upon to discriminate between closely similar compounds.

The correlation between telomerase inhibition and calculated binding energies has been explored in Figure 3. In general, the predicted energies unambiguously indicate the most and least potent compounds. This is very apparent for the subset of 10 3,6,9-trisubstituted molecules with anilino groups at the 9-position (Figure 3a), where the correlation coefficient is 0.86. Other subsets (Figure 3b,c) show some outliers, but the trends are still apparent even though the relationships are flatter than for the set in Figure 3a.

Semiempirical quantum chemistry calculations have been performed on the 9-anilino protonated acridine molecule as a model for the compounds with this substitution and on the 3′ G-quartet plane. The electrostatic potential generated at the optimal 9-anilino acridine low-energy conformation for interacting with the quadruplex, shown in Figure 5a, indicates the presence of two electron-deficient regions in the molecule. The first one is related to the acridinium ring nitrogen, whereas the second one is related to the anilinium proton. Docking experiments showed that these two electron-poor regions directly interact with two electron-rich regions present in the G-quartet plane: the central O6 channel and the region between the N3, C2, and N2 atoms in an individual guanine base (see Figure 5b). Electron-withdrawing substituents on the phenyl aromatic ring increase the partial positive charge on the anilino proton, leading to a lower binding energy and to more potent telomerase inhibition. The efficiency of the substituent electronic effect is shown by the substituent Hammett values (Figure 6) correlating well with the $^{tel}EC_{50}$ data (this is only appropriate for substituents with no hydrogen bonding ability because the formation of hydrogen bond(s) between ligand and quadruplex would affect the correlation). This is shown by compound **12**, which is one of the most active compounds even though this anilino substitutent is electron-donating. Conformational searches showed that the introduction of a NH_2 in the ortho position of the anilino ring was ideal for the formation of a

hydrogen bond with an adjacent guanine, enhancing the affinity of the drug toward the G-quadruplex structure.

Discussion

The trisubstituted acridine compounds reported here all belong to a group of DNA binding agents with, in principle, the ability to bind to the intramolecular quadruplex DNA formed by the G-rich single-stranded overhang of telomeric DNA, coupled with lower affinity to duplex DNA. An acridine pharmacophore was postulated at the outset of these studies[27] to be an appropriate building block for this type of agent. This is due in part to the ability of the acridine to be protonated at physiological pH, thus providing increased stabilization by acting as a pseudocation, and in part to the additional stabilization afforded by nonbonded interactions with substituents in the quadruplex grooves. The former property would complement the ion channel that runs along the central region of a DNA quadruplex, at the center of individual G-quartets. We have previously described acridine derivatives with disubstitution where the ligands are directed toward two of the four grooves formed in the quadruplex.[19] These derivatives possess telomerase inhibitory values of at most 1−5 μM, with acute cytotoxicity at similar levels. We find now that a number of derivatives, with a range of substituents at the 9-position, show potent telomerase inhibition that is a significant improvement over the initial two anilino compounds and at the same time show only modest acute cytotoxicity.

This study has shown that the 3,6,9-trisubstituted compounds are the most potent of the three regioisomeric series examined and that this behavior can be rationalized on the basis of differences in predicted binding to the intramolecular human quadruplex structure. These correlations, together with the solution binding data, provide further support for the proposed mechanism of action of these compounds being quadruplex-mediated inhibition of telomerase function. The findings that these and other G-quadruplex-binding ligands produce cellular senescence[22b,28,32] in time scales much less than would be expected from the classic model of telomere attrition suggest to us that formation of a G-quadruplex complex may be occurring at the extreme end of single-strand telomere overhangs such that noncatalytic functions of telomerase such as end-capping of the telomere may also be compromised over a short time scale. We suggest that formation of a G-quadruplex complex would result in disruption of the D- and t-loops, exposing the extreme 3′ telomere ends and triggering the onset of senescence.[33] It is also possible that there exists a subpopulation of short telomeric-containing cells within a population of heterogeneous telomere lengths, which may be especially sensitive to telomere-shortening agents and thus to senescence.[34] In vivo studies on G-quadruplex ligands have not yet been extensively reported, although activity has been found[28] for compound **7** in the present series. It is encouraging for future studies in *Homo sapiens* that the ALT pathway may not be of functional significance[35] as a potential mechanism of resistance to anti-telomerase agents.

As yet, no experimental structural data are available on G-quadruplex ligands binding to the intramolecular structure(s) likely to be formed by human telomeric DNA sequences, so molecular modeling studies such as those reported here are still conjectural. However, they are supported in broad terms by several NMR studies on model systems[21a,36] that consistently agree in finding that the ligands bind at the end of the stack of G-quartets in a quadruplex. Such an arrangement has also been found in a recent crystal-structure analysis[37] from this laboratory of a complex between compound **44** and the dimeric *Oxytricha* quadruplex. This structure shows in addition that the 3- and 6-substituent side chains attached to the acridine chromophore do reside in the quadruplex grooves, making close contacts with atoms forming the groove, in accord with features seen in the molecular modeling studies. The assumption here that the ligands bind to the 3′ external face of a G-quartet is in accord with the position of the bound drug molecules in the crystal structure of a complex between daunomycin and the parallel quadruplex d(TGGGGT).[38]

Experimental Section

Synthetic Chemistry. Melting points (mp) were recorded on a Leica Galen III hot-stage melting point apparatus and are uncorrected. NMR spectra were recorded at 250 MHz on a Bruker AC250 spectrometer in either Me_2SO-d_6 or $CDCl_3$ solution at 303 ± 1 K using Me_4Si as internal standard. EI (70 eV), FAB, and high-resolution accurate mass spectra were determined by The School of Pharmacy, University of London (U.K). Elemental analyses were carried out by Medac Ltd. (Brunel Science Center, Egham, Surrey, U.K.); results for elements indicated by symbols were within ±0.4% of theoretical values. TLC was carried out on silica gel (Merck 60F-254) using $CHCl_3$−MeOH (0−20% MeOH) as eluent, with visualization at 254 and 366 nm. Organic solutions were dried over sodium sulfate.

3,6-Bis(3-pyrrolidin-1-ylpropionamido)-9-chloroacridine (4). 3,6-Bisamidoacridone **1** (5.00 g, 10 mmol) was treated with refluxing $POCl_3$ (75 mL) for 3 h. The reaction mixture was cooled to 0 °C, and anhydrous diethyl ether was added to precipitate product. Solids were filtered from the solution and washed with ether (2 × 20 mL). The solid was redissolved in $CHCl_3$ (100 mL) and H_2O (100 mL) and made basic with dilute ammonia. The organic phase was collected, washed with brine (50 mL), and evaporated to dryness to give the desired product **4** (4.9 g, 94%) as a green solid. ^{1}H NMR ($CDCl_3$): δ 1.97 (8 H, m, $N(CH_2CH_2)_2$), 2.62 (4 H, t, J = 6.3 Hz, $COCH_2CH_2N$), 2.75 (8 H, m, $N(CH_2CH_2)_2$), 2.92 (4 H, t, J = 6.3 Hz, $COCH_2CH_2N$), 7.79 (2 H, dd, J = 2.1 Hz, J = 9.3 and 2.2 Hz, H-2,7), 8.10 (2H, d, J = 2.1 Hz, H-4,5), 8.33 (2 H, d, J = 9.4 Hz, H-1,8), 11.72 (2 H, s, NHCO). MS, m/z: 494.2342 ($C_{27}H_{33}ClN_5O_2$ M + H requires 494.2323).

2,6-Bis(3-pyrrolidin-1-ylpropionamido)-9-chloroacridine (5). 2,6-Bisamidoacridone **2** (2.00 g, 4.2 mmol) was treated with refluxing $POCl_3$ (50 mL) for 3 h. The reaction mixture was cooled to 0 °C, and anhydrous diethyl ether was added to precipitate product. Solids were filtered from the solution and washed with ether (2 × 20 mL). The solid was redissolved in $CHCl_3$ (100 mL) and H_2O (100 mL) and made basic with dilute ammonia. The organic phase was collected, washed with brine (50 mL), and evaporated to dryness to give the desired product **5** (1.3 g, 62%) as a light-brown solid. ^{1}H NMR ($CDCl_3$): δ 1.97−1.98 (8 H, m, $N(CH_2CH_2)_2$), 2.61−2.66 (4 H, m, $COCH_2CH_2N$), 2.75−2.76 (8 H, m, $N(CH_2CH_2)_2$), 2.90−2.96 (4 H, m, $COCH_2CH_2N$), 7.66−7.70 (1 H, d, J = 9.3 and 2.2 Hz, H-3/7), 7.92−7.96 (1H, d, J = 9.3 and 2.2 Hz, H-3/7), 8.08−8.11 (1 H, d, J = 9.3 Hz, H-4/8), 8.17−8.18 (1 H, m, H-1/5), 8.31−8.35 (1 H, d, J = 9.3 Hz, H-4/8), 8.75−8.76 (1 H, m, H-1/5), 11.72 (2 H, s, NHCO). MS, m/z: 494.2342 ($C_{27}H_{33}ClN_5O_2$ M + H requires 494.2323).

2,7-Bis(3-pyrrolidin-1-ylpropionamido)-9-chloroacridine (6). 2,7-Bisamidoacridone **3** (1.00 g, 2.1 mmol) was

treated with refluxing $POCl_3$ (50 mL) for 3 h. The reaction mixture was cooled to 0 °C, and anhydrous diethyl ether was added to precipitate product. Solids were filtered from the solution and washed with ether (2 × 20 mL). The solid was redissolved in $CHCl_3$ (100 mL) and H_2O (100 mL) and made basic with dilute ammonia. The organic phase was collected, washed with brine (50 mL), and evaporated to dryness to give the desired product **6** (750 mg, 72%) as a yellow solid. Mp >320 °C. ^{1}H NMR ($CDCl_3$): δ 1.91 (8 H, m, $N(CH_2CH_2)_2$), 2.56 (4 H, t, J = 5.8 Hz, $COCH_2CH_2N$), 2.69 (8 H, m, $N(CH_2CH_2)_2$), 2.86 (4 H, t, J = 5.8 Hz, $COCH_2CH_2N$), 7.64 (2 H, dd, J = 9.3 Hz, J = 2.0 Hz, H-3,6), 8.05 (2 H, d, J = 9.3 Hz, H-4,5), 8.64 (2 H, d, J = 2.0 Hz, H-1,8), 11.78 (2 H, s, NHCO). MS, *m*/*z*: 494.2342 ($C_{27}H_{33}ClN_5O_2$ M + H requires 494.2323).

9-Substitution General Procedure. To a vigorously stirred solution of the 3,6-bisamido-9-chloroacridine in $CHCl_3$ was added dropwise a solution of the proposed substituent amine in $CHCl_3$. This solution was then stirred under reflux for 2 h, the solvent was removed under reduced pressure, and the resultant solid was washed with EtOH and Et_2O to give the desired trisubstituted derivative. Hydrochloride salts were prepared by adding saturated ethereal HCl to a solution of the free base in chloroform, collecting the precipitated product, and washing with dry ether and hexane.

3,6-Bis(3-pyrrolidin-1-ylpropionamido)-9-(4-dimethylaminophenylamino)acridine (7). 3,6-Bisamido-9-chloroacridine **4** (400 mg, 0.8 mmol) was treated with *N*,*N*-dimethylaminoaniline (0.4 mL) according to the general procedure to give the desired product **7** (400 mg, 88%) as a pale-brown solid. Mp >320 °C. ^{1}H NMR ($CDCl_3$): δ 1.81 (8 H, m, $N(CH_2CH_2)_2$), 2.74 (4 H, t J = 6.7 Hz, $COCH_2CH_2N$), 2.85 (8 H, m, $N(CH_2CH_2)_2$), 2.93 (6 H, s, $N(CH_3)_2$), 3.07 (4 H, t, J = 6.7 Hz, $COCH_2CH_2N$), 6.78 (2 H, d, J = 8.9 Hz, H-2,7), 6.99 (2 H, d, J = 8.9 Hz, H-1,8), 7.20 (2 H, d, J = 9.1 Hz, H-3′,5′), 7.97 (2 H, d, J = 9.1 Hz, H-2′,6′), 8.24 (2H, s, H-4, 5) 10.92 (2 H, s, NHCO). MS, *m*/*z*: 594.3540 ($C_{35}H_{40}N_7O_2$ M + H requires 594.3556).

3,6-Bis(3-pyrrolidin-1-ylpropionamido)-9-(4-aminophenylamino)acridine (8). 3,6-Bisamido-9-chloroacridine **4** (400 mg, 0.8 mmol) was treated with 1,4-phenylenediamine (0.5 mL) according to the general procedure to give the desired product **8** (410 mg, 90%) as a brown solid. Mp >320 °C. ^{1}H NMR ($CDCl_3$): δ 1.81 (8 H, m, $N(CH_2CH_2)_2$), 2.81 (4 H, t, J = 6.9 Hz, $COCH_2CH_2N$), 2.85 (8 H, m, $N(CH_2CH_2)_2$), 3.16 (4 H, t, J = 6.9 Hz, $COCH_2CH_2N$), 6.67 (2 H, d, J = 8.7 Hz, H-2,7), 6.96 (2 H, d, J = 8.7 Hz, H-1,8), 7.26 (2 H, d, J = 8.6 Hz, H-3′,5′), 8.03 (2 H, d, J = 8.6 Hz, H-2′,6′), 8.34 (2H, s, H-4, 5), 10.92 (2 H, s, NHCO). MS, *m*/*z*: 566.3260 ($C_{33}H_{44}N_7O_2$ M + H requires 566.3260).

3,6-Bis(3-pyrrolidin-1-ylpropionamido)-9-(3-(dimethylamino)propylamino)acridine (9). 3,6-Bisamido-9-chloroacridine **4** (500 mg, 1.0 mmol) was treated with *N*,*N*-dimethylpropylenediamine (0.4 mL) according to the general procedure to give the desired product **9** (390 mg, 70%) as a pale-brown solid. ^{1}H NMR ($CDCl_3$): δ 1.86 (10 H, m, $N(CH_2CH_2)_2$, $HNCH_2CH_2CH_2NMe_2$), 2.29 (6 H, s, $N(CH_3)_2$), 2.49−2.55 (6 H, m, $COCH_2CH_2N$, $HNCH_2CH_2CH_2NMe_2$), 2.63 (8 H, m, $N(CH_2CH_2)_2$), 2.79−2.83 (4 H, m, $COCH_2CH_2N$), 3.74−3.78 (2 H, t, J = 5.6 Hz, $HNCH_2CH_2CH_2NMe_2$), 7.61−7.62 (2 H, d, J = 1.9 Hz, H-4,5), 7.84−7.88 (2 H, dd, J = 9.3 and 1.9 Hz, H-2,7), 8.00−8.03 (2 H, d, J = 9.3 Hz, H-1,8), 11.49 (2 H, s, NHCO). MS, *m*/*z*: 560.3730 ($C_{32}H_{46}N_7O_2$ M + H requires 560.3713).

3,6-Bis(3-pyrrolidin-1-ylpropionamido)-9-(2-piperidin-1-ylethylamino)acridine (10). 3,6-Bisamido-9-chloroacridine **4** (500 mg, 1.0 mmol) was treated with 1-(2-aminoethyl)-piperidine (0.4 mL) according to the general procedure to give the desired product **10** (210 mg, 36%) as an orange solid. ^{1}H NMR ($CDCl_3$): δ 1.54−1.56 (2 H, m, $N(CH_2CH_2)_2CH_2$), 1.68−1.72 (4 H, m, $N(CH_2CH_2)_2CH_2$), 1.94−1.96 (8 H, m, $N(CH_2CH_2)_2$), 2.43−2.44 (4 H, m, $N(CH_2CH_2)_2CH_2$), 2.59−2.68 (6 H, m, $COCH_2CH_2N$ and $HNCH_2CH_2N$), 2.73 (8 H, m, $N(CH_2CH_2)_2$), 2.88−2.93 (4 H, m, $COCH_2CH_2N$), 3.85−3.89 (2 H, m, $HNCH_2CH_2N$), 6.76 (1 H, s, NH), 7.67 (2 H, d, J = 2.0 Hz, H-4,5), 7.98−8.02 (2 H, dd, J = 9.4 and 2.0 Hz, H-2,7), 8.12−8.16 (2 H, d, J = 9.4 Hz, H-1,8), 11.58 (2 H, s, NHCO). MS, *m*/*z*: 586.3845 ($C_{34}H_{48}N_7O_2$ M + H requires 586.3869). Found, HCl salt: C 51.65, H 7.16, N 12.08%. Calcd (anhydrous $C_{34}H_{47}N_7O_2$·4HCl·3.0 mol of H_2O): C 51.98, H 7.31, N 12.48%.

3,6-Bis(3-pyrrolidin-1-ylpropionamido)-9-(3-aminophenylamino)acridine (11). 3,6-Bisamido-9-chloroacridine **4** (500 mg, 1.0 mmol) was treated with 1,3-phenylenediamine (0.5 mL) according to the general procedure to give the desired product **11** (446 mg, 78%) as an orange solid. Mp >320 °C. ^{1}H NMR ($CDCl_3$): δ 1.94 (8 H, m, $N(CH_2CH_2)_2$), 2.62 (4 H, t, J = 6.5 Hz, $COCH_2CH_2N$), 2.72 (8 H, m, $N(CH_2CH_2)_2$), 2.89 (4 H, t, J = 6.5 Hz, $COCH_2CH_2N$), 3.62 (2 H, sbr, NH_2), 6.12 (1 H, m, H-5′), 6.21 (1 H, s, H-2′), 6.34 (2 H, m, H-4′,6′), 6.96 (2 H, m, H-4,5), 7.99 (4 H, m, H-1,2,7,8). MS, *m*/*z*: 566.3219 ($C_{33}H_{40}N_7O_2$ M + H requires 566.3243). Found: C 67.07; H 7.06, N 16.59%. Calcd ($C_{33}H_{39}N_7O_2$·1.2 mol of H_2O): C 67.48, H 7.10, N 16.69%.

3,6-Bis(3-pyrrolidin-1-ylpropionamido)-9-(2-aminophenylamino)acridine (12). 3,6-Bisamido-9-chloroacridine **4** (500 mg, 1.0 mmol) was treated with 1,2-phenylenediamine (0.5 mL) according to the general procedure to give the desired product **12** (400 mg, 88%) as an orange solid. Mp >320 °C. ^{1}H NMR ($CDCl_3$): δ 1.90 (8 H, m, $N(CH_2CH_2)_2$), 2.4 (8 H, m, $N(CH_2CH_2)_2$), 2.55 (4 H, m, $COCH_2CH_2N$), 2.68 (4 H, m, $COCH_2CH_2N$), 3.49 (2 H, sbr, NH_2), 6.80 (6 H, m, 4Ar-H, H-1,8), 7.95 (4 H, m, H-2,4,5,7). MS, *m*/*z*: 566.3219 ($C_{33}H_{40}N_7O_2$ M + H requires 566.3243). Found: C 66.67, H 7.09, N 16.49%. Calcd ($C_{33}H_{39}N_7O_2$·1.4 mol of H_2O): C 67.07, H 7.13, N 16.59%.

3,6-Bis(3-pyrrolidin-1-ylpropionamido)-9-(3-(dimethylamino)phenylamino)acridine (13). 3,6-Bisamido-9-chloroacridine **4** (500 mg, 1.0 mmol) was treated with *N*,*N*-dimethyl-1,3-phenylenediamine (0.5 mL) according to the general procedure to give the desired product **13** (400 mg, 88%) as a brown solid. Mp >320 °C. ^{1}H NMR ($CDCl_3$): δ 1.91 (8 H, m, $N(CH_2CH_2)_2$), 2.60 (4 H, m, $COCH_2CH_2N$), 2.67 (8 H, m, $N(CH_2CH_2)_2$), 2.88 (6 H, s, $N(CH_3)_2$), 2.90 (4 H, m, $COCH_2$-CH_2N), 6.14 (1 H, d, J = 7.9 Hz, H-4′), 6.30 (1 H, s, H-2′), 6.39 (1 H, d, J = 8.1 Hz, H-6′), 7.11 (1 H, dd, J = 7.9 and 8.1 Hz, H-5′), 7.9 (6 H, m, H-1,2,4,5,7,8), 11.58 (2 H, s, NHCO). MS, *m*/*z*: 594.3572 ($C_{35}H_{43}N_7O_2$ M + H requires 594.3556). Found: C 66.62, H 6.9, N 15.54%. Calcd ($C_{35}H_{42}N_7O_2$·2.0 mol of H_2O): C 66.86, H 7.37, N 15.59%.

3,6-Bis(3-pyrrolidin-1-ylpropionamido)(9-cyclohexylamino)acridine (14). 3,6-Bisamido-9-chloroacridine **4** (500 mg, 1.0 mmol) was treated with cyclohexylamine (0.5 mL) according to the general procedure to give the desired product **14** (484 mg, 86%) as yellow solid. Mp >300 °C. ^{1}H NMR ($CDCl_3$): δ 1.23 (14 H, m, CH_2), 1.68 (2 H, m, CH_2), 1.76 (4 H, m, CH_2), 1.92 (2 H, m, CH_2), 2.12 (4 H, m, CH_2), 2.5 (4 H, m, CH_2), 2.88 (4 H, m, CH_2), 3.06 (1 H, m, CH), 3.83 (1 H, sbr, NH), 7.78 (2 H, d, J = 8.8 Hz, H-2,7), 7.96 (2 H, s, H-4,5), 7.97 (2 H, d, J = 8.8 Hz, H-1,8), 11.38 (2 H, sbr, NHCO). MS, *m*/*z*: 556.3534 ($C_{33}H_{45}N_6O_2$ M + H requires 556.3526). Found: C 68.60, H 7.97, N 14.54%. Calcd ($C_{33}H_{44}N_6O_2$·1.2 mol of H_2O): C 67.48, H 8.09, N 14.53%.

3,6-Bis(3-pyrrolidin-1-ylpropionamido)-9-(2-methoxyethylamino)acridine (15). 3,6-Bisamido-9-chloroacridine **4** (500 mg, 1.0 mmol) was treated with 2-methoxyethylamine (0.5 mL) according to the general procedure to give the desired product **15** (290 mg, 54%) as a brown solid. Mp <100 °C. ^{1}H NMR (DMSO): δ 1.88 (8 H, m, $N(CH_2CH_2)_2$), 2.65 (6 H, m, $COCH_2CH_2N$ and $HNCH_2CH_2OMe$), 2.68 (8 H, m, $N(CH_2$-$CH_2)_2$), 2.87−2.92 (4 H, m, $COCH_2CH_2N$), 47.2 (5 H, m, $HNCH_2CH_2OCH_3$), 7.59 (2 H, d, J = 1.9 Hz, H-4,5), 7.94−7.99 (2 H, dd, J = 9.4 and 1.9 Hz, H-2,7), 8.05−8.08 (2 H, d, J = 9.4 Hz, H-1,8), 11.54 (2 H, s, NHCO). MS, *m*/*z*: 533.3231 ($C_{30}H_{41}N_6O_3$ M + H requires 533.3240).

3,6-Bis(3-pyrrolidin-1-ylpropionamido)(9-cycloheptylamino)acridine (16). 3,6-Bisamido-9-chloroacridine **4** (500 mg, 1.0 mmol) was treated with cycloheptylamine (0.5 mL) according to the general procedure to give the desired product **16** (485 mg, 84%) as a yellow solid. Mp >320 °C. ^{1}H NMR ($CDCl_3$): δ 1.62 (16 H, m, CH_2), 2.1 (4 H, m, CH_2), 2.43 (4 H,

m, CH_2), 2.55 (4 H, m, $J = 5.0$ Hz, CH_2), 2.70 (4 H, m, $J = 5.0$ Hz, CH_2), 2.92 (1 H, t, $J = 5.1$ Hz, CH), 4.08 (1 H, sbr, NH), 7.92 (2 H, m, H-2,7), 8.33 (4 H, m, H-1,4,5,8). MS, *m*/*z*: 571.3735 ($C_{34}H_{47}N_6O_2$ M + H requires 571.3761).

3,6-Bis(3-pyrrolidin-1-ylpropionamido)-9-(4-acetylphenylamino)acridine (17). 3,6-Bisamido-9-chloroacridine **4** (500 mg, 1.0 mmol) was treated with 4-aminoacetophenone (0.5 mL) according to the general procedure to give the desired product **17** (400 mg, 88%) as an orange solid. Mp >320 °C. ^{1}H NMR ($CDCl_3$): δ 1.69 (8 H, m, $N(CH_2CH_2)_2$), 2.18 (7 H, m, $COCH_2CH_2N$, $COCH_3$), 2.51 (8 H, m, $N(CH_2CH_2)_2$), 2.76 (4 H, m, $COCH_2CH_2N$), 6.81 (2 H, d, $J = 7.9$ Hz, 2-ArH), 6.90 (2 H, d, $J = 7.9$ Hz, 2-ArH), 7.88 (2 H, d, H-2,7), 8.10 (4 H, m, H-1,4,5,8), 10.36 (2 H, sbr, NHCO).

3,6-Bis(3-pyrrolidin-1-ylpropionamido)-9-(2-(dimethylamino)ethylamino)acridine (18). 3,6-Bisamido-9-chloroacridine **4** (500 mg, 1.0 mmol) was treated with *N*,*N*-dimethylethylenediamine (0.03 mL) according to the general procedure to give the desired product **18** (370 mg, 67%) as a yellow solid. ^{1}H NMR ($CDCl_3$): δ 1.88−1.95 (8 H, m, $N(CH_2CH_2)_2$), 2.42 (6 H, s, $N(CH_3)_2$), 2.58−2.68 (6 H, m, $COCH_2CH_2N$ and $HNCH_2CH_2NMe_2$), 2.72 (8 H, m, $N(CH_2CH_2)_2$), 2.87−2.92 (4 H, m, $COCH_2CH_2N$), 4.06−4.10 (2 H, t, $J = 5.6$ Hz, $HNCH_2CH_2NMe_2$), 7.59 (2 H, d, $J = 1.9$ Hz, H-4,5), 7.94−7.99 (2 H, dd, $J = 9.4$ and 1.9 Hz, H-2,7), 8.05−8.08 (2 H, d, $J = 9.4$ Hz, H-1,8), 11.54 (2 H, s, NHCO). MS, *m*/*z*: 546.3570 ($C_{31}H_{44}N_7O_2$ M + H requires 546.3556). Found, HCl salt: C 49.98, H 6.98, N 13.16%. Calcd (anhydrous $C_{31}H_{43}N_7O_2$·4HCl·3.0 mol of H_2O): 49.94, H 7.16, N 13.15%.

3,6-Bis(3-pyrrolidin-1-ylpropionamido)-9-[2-(1-methylpyrrolidin-2-yl)ethylamino]acridine (19). 3,6-Bisamido-9-chloroacridine **4** (0.5 mg, 1.0 mmol) was treated with 2-(2-aminoethyl)-1-methylpyrrolidine (0.43 mL) according to the general procedure to give the desired product **19** (380 mg, 64%) as a yellow solid. ^{1}H NMR ($CDCl_3$): δ 1.76−1.89 (4 H, m, $MeN(CH_2CH_2CH_2CH-)$, 1.96 (10 H, m, $N(CH_2CH_2)_2$ and $HNCH_2CH_2-$), 2.08−2.28 (2 H, m, $MeN(CH_2CH_2CH_2CH-)$, 2.51 (3 H, s, NCH_3), 2.58−2.63 (4 H, t, $J = 5.3$ Hz, $COCH_2CH_2N$), 2.72, (8 H, m, $COCH_2CH_2N$), 2.88−2.92 (4 H, m, t, $J = 5.3$ Hz, $COCH_2CH_2N$), 3.23−3.29 (1 H, m, $MeN(CH_2CH_2CH_2CH)$, 4.09−4.20 (2 H, m, $HNCH_2CH_2-$), 7.58−7.59 (2 H, d, $J = 2.0$ Hz, H-4,5), 7.96−8.02 (2 H, m, H-2,7), 8.05−8.09 (2 H, m, $J = 9.4$ Hz, H-1,8), 8.39 (1 H, s, NH), 11.55 (2 H, s, NHCO). MS, *m*/*z*: 586.3840, ($C_{34}H_{48}N_7O_2$ M + H requires 586.3869). Found, HCl salt: C 49.80, H 7.39, N 12.23%. Calcd ($C_{34}H_{47}N_7O_2$·4HCl·5.0 mol of H_2O): C 49.70, H 7.48, N 11.93%.

3,6-Bis(3-pyrrolidin-1-ylpropionamido)-9-[(pyridin-3-ylmethyl)amino]acridine (20). 3,6-Bisamido-9-chloroacridine **4** (500 mg, 1.0 mmol) was treated with pyridin-3-ylmethylamine (0.31 mL) according to the general procedure to give the desired product **20** (220 mg, 39%) as a yellow solid. ^{1}H NMR ($CDCl_3$): δ 1.85 (8 H, m, $N(CH_2CH_2)_2$), 2.48−2.53 (4 H, dd, $J = 5.3$ and 6.0 Hz, $COCH_2CH_2N$), 2.63 (8 H, m, $N(CH_2CH_2)_2$), 2.78−2.83 (4 H, dd, $J = 5.3$ and 6.0 Hz, $COCH_2CH_2N$), 4.91 (2 H, s, $HNCH_2$-aryl), 7.18−7.23 (1 H, m, H-5′), 7.62−7.65 (2 H, m, H-2, 7), 7.76 (2 H, m, H-4, 5), 7.91−7.95 (2 H, d, $J = 9.2$ Hz, H-1,8), 8.49−8.50 (2 H, m, H-4′, 6′), 8.62 (1 H, s, H-2′), 11.57 (2 H, s, NHCO). MS, *m*/*z*: 566.3226 (requires $C_{33}H_{40}N_7O_2$ M + H 566.3243).

3,6-Bis(3-pyrrolidin-1-ylpropionamido)-9-(3-acetylaminophenylamino)acridine (21). 3,6-Bisamido-9-chloroacridine **4** (500 mg, 1.0 mmol) was treated with *N*-(3-aminophenyl)-acetamide (0.5 g) according to the general procedure to give the desired product **21** (430 mg, 70%) as a yellow solid. ^{1}H NMR (DMSO): δ 1.89−2.07 (11 H, m, $N(CH_2CH_2)_2$ and CH_3), 3.05−3.10 (8 H, m, $N(CH_2CH_2)_2$), 3.39−3.53 (8 H, m, $COCH_2CH_2N$), 6.97−7.00 (1 H, d, $J = 7.8$ Hz, H-6′), 7.34−7.39 (1 H, t, $J = 7.8$ Hz, H-5′), 7.43−7.47 (2 H, d, $J = 9.4$ Hz, H-2, 7), 7.51−7.54 (1 H, d, $J = 7.8$ Hz, H-4′), 7.79 (1 H, s, H-2′), 8.11−8.15 (2 H, d, $J = 9.4$ Hz, H-1, 8), 8.50 (2 H, s, H-4, 5), 10.35 (1 H, s, NH), 11.07 (2 H, s, NH), 11.17 (1 H, s, NH), 11.38 (2 H, s, NH), 14.08 (1 H, s, NH).

3,6-Bis(3-pyrrolidin-1-ylpropionamido)(9-cyclopropylamino)acridine (22). 3,6-Bisamido-9-chloroacridine **4** (300 mg, 0.6 mmol) was treated with cyclopropylamine (0.43 g, 1.8 mmol) according to the general procedure to give the desired product **22** (290 mg, 70%) as a yellow solid. Mp >320 °C. ^{1}H NMR (DMSO): δ 0.36 (2 H, m, CH_2), 0.39 (2 H, m, CH_2), 1.70 (8 H, m, $N(CH_2CH_2)_2$), 2.55 (4 H, m, $COCH_2CH_2N$), 2.58 (8 H, m, $N(CH_2CH_2)_2$), 2.84 (4 H, m, $COCH_2CH_2N$), 2.90 (1 H, m, CH), 7.02 (2 H, m, H-1,8), 7.9 (2 H, m, H-4,5), 8.2 (6 H, m, H-2,7), 10.00 (1 H, s, NHCO), 10.28 (2 H, s, NHCO). MS, *m*/*z*: 515.3160 ($C_{30}H_{39}N_6O_2$ M + H requires 515.3134).

3,6-Bis(3-pyrrolidin-1-ylpropionamido)-9-(4-fluorophenylamino)acridine (23). 3,6-Bisamido-9-chloroacridine **4** (500 mg, 1.0 mmol) was treated with 4-fluoroaniline (0.3 mL) according to the general procedure to give the desired product **23** (650 mg, 71%) as a red solid. ^{1}H NMR ($CDCl_3$): δ 1.89 (8 H, bs, $N(CH_2CH_2)_2$), 2.59 (4 H, t, $J = 5.5$ Hz, $COCH_2CH_2N$), 2.68 (8 H, bs, $N(CH_2CH_2)_2$), 2.86 (4 H, t, $J = 5.5$ Hz, $COCH_2CH_2N$), 6.80 (4 H, m, H-2,7 and H-3′,5′), 6.98 (4 H, m, H-1,8 and H-2′,6′), 8.02 (2H, s, H-4,5), 11.57 (2H, s, NHCO). MS, *m*/*z*: 569.3056 ($C_{33}H_{38}FN_6O_2$ M + H requires 569.3040). Found, HCl salt: C 55.06, H 6.11, N 11.75%. Calcd (anhydrous $C_{33}H_{37}N_7O_2$·3HCl·3.0 mol of H_2O): C 55.06, H 6.11, N 11.75%.

3,6-Bis(3-pyrrolidin-1-ylpropionamido)-9-(2-methylsulfanylphenylamino)acridine (24). 3,6-Bisamido-9-chloroacridine **4** (500 mg, 1.0 mmol) was treated with 2-(methylthio)-aniline (0.2 mL) according to the general procedure to give the desired product **24** (650 mg, 71%) as a red solid. Mp >320 °C. ^{1}H NMR (DMSO): δ 1.9 (8 H, m, $N(CH_2CH_2)_2$), 2.39 (3 H, s, SMe), 2.42 (8 H, m, $N(CH_2CH_2)_2$), 2.56 (4 H, m, $COCH_2CH_2N$), 2.84 (4 H, m, $COCH_2CH_2N$), 6.14 (1 H, d, $J = 7.9$ Hz, H-4′), 6.30 (1 H, s, H-2′), 6.39 (1 H, d, $J = 8.1$ Hz, H-6′), 7.11 (1 H, dd, $J = 7.9$ and 8.1 Hz, H-5′), 7.9 (6 H, m, H-1,2,4,5,7,8), 11.58 (2 H, s, NHCO). MS, *m*/*z*: 597.3035 ($C_{34}H_{41}N_6O_2$ M + H requires 597.3012).

3,6-Bis(3-pyrrolidin-1-ylpropionamido)-9-(3-methylsulfanylphenylamino)acridine (25). 3,6-Bisamido-9-chloroacridine **4** (800 mg, 1.6 mmol) was treated with 3-(methylthio)-aniline (0.4 mL) according to the general procedure to give the desired product **25** (650 mg, 71%) as a red solid. Mp >320 °C. ^{1}H NMR (DMSO): δ 1.9 (8 H, m, $N(CH_2CH_2)_2$), 2.39 (3 H, s, SMe), 2.42 (8 H, m, $N(CH_2CH_2)_2$), 2.56 (4 H, m, $COCH_2CH_2N$), 2.84 (4 H, m, $COCH_2CH_2N$), 6.61 (1 H, m, H-4′), 6.79 (1 H, s, H-2′), 6.85 (1 H, m, H-6′), 7.10 (3 H, m, H-1,8, H-5′), 7.95 (4 H, m, H-2,4,5,7), 11.37 (2 H, S, NHCO). MS, *m*/*z*: 597.3035 ($C_{34}H_{41}N_6O_2$ M + H requires 597.3012).

2,6-Bis(3-pyrrolidin-1-ylpropionamido)-9-(4-aminophenylamino)acridine (26). 2,6-Bisamido-9-chloroacridine **5** (500 mg, 1.0 mmol) was treated with 1,4-phenylenediamine (0.5 mL) according to the general procedure to give the desired product **26** (400 mg, 88%) as a brown solid. Mp >320 °C. ^{1}H NMR ($CDCl_3$): δ 1.83 (8 H, m, $N(CH_2CH_2)_2$), 2.55 (4 H, m, $COCH_2CH_2N$), 2.58 (8 H, m, $N(CH_2CH_2)_2$), 2.84 (4 H, m, $COCH_2CH_2N$), 6.61 (2 H, d, $J = 8.7$ Hz, ArH-3′,5′), 6.66 (2 H, d, $J = 8.7$ Hz, ArH-2′,6′), 7.5−8.0 (6 H, m, H-1,3,4,5,7,8), 10 (1 H, s, NHCO), 10.89 (1 H, s, NHCO). MS, *m*/*z*: 566.3219 ($C_{33}H_{44}N_7O_2$ M + H requires 566.3243).

2,6-Bis(3-pyrrolidin-1-ylpropionamido)-9-(4-(dimethylamino)phenylamino)acridine (27). 2,6-Bisamido-9-chloroacridine **5** (500 mg, 1.0 mmol) was treated with 4-*N*,*N*-dimethylaminoaniline (0.4 g) according to the general procedure to give the desired product **27** (210 mg, 36%) as a dark-brown solid. ^{1}H NMR (DMSO): δ 1.87−1.92 (8 H, m, $N(CH_2CH_2)_2$), 2.38−2.59 (4 H, m, $COCH_2CH_2N$), 2.61−2.80 (8 H, m, $N(CH_2CH_2)_2$), 2.87−2.92 (10 H, m, $COCH_2CH_2N$ and $N(CH_3)_2$), 6.64−6.67 (2 H, d, $J = 9.0$ Hz, H-2′, 6′ or H-3′, 5′), 6.91−6.94 (2H, d, $J = 9.0$ Hz, H-2′, 6′ or H-3′, 5′), 7.49−7.52 (1 H, m, $J = 9.0$ Hz, acridine), 7.60−7.64 (1 H, m, acridine), 7.73−7.76 (1 H, m, acridine), 7.91−7.92 (2 H, m, acridine), 8.40 (1 H, s, acridine), 11.33 (1 H, s, NHCO), 11.53 (1 H, s, NHCO). MS, *m*/*z*: 594.3540 ($C_{35}H_{44}N_7O_2$ M + H requires 594.3556).

2,6-Bis(3-pyrrolidin-1-ylpropionamido)-9-(2-(dimethylamino)ethylamino)acridine (28). 2,6-Bisamido-9-chloroacridine **5** (500 mg, 1.0 mmol) was treated with *N*,*N*-dimethylethylamine (0.33 mL) according to the general procedure to give the desired product **28** (410 mg, 75%) as a

brown hygroscopic solid. ^{1}H NMR ($CDCl_3$): δ 1.95 (8 H, m, $N(CH_2CH_2)_2$), 2.39 (6 H, s, CH_3), 2.61−2.67 (6 H, m, $COCH_2$-CH_2N and $HNCH_2CH_2N$), 2.72 (8 H, s, $N(CH_2CH_2)_2$), 2.88−2.94 (4 H, m, $COCH_2CH_2N$), 3.91−3.96 (2 H, m, $HNCH_2CH_2N$), 7.32−7.33 (1 H, m, H-3/7), 7.78−7.79 (1H, m, H-3/7), 7.93−8.00 (2 H, m, H-8, 1), 8.06−8.10 (1 H, m, J = 9.4 Hz, H-4), 8.96−8.97 (1 H, m, H-5), 11.54−11.62 (2 H, s, NHCO). MS, *m*/*z*: 546.3580 ($C_{31}H_{44}N_7O_2$ M + H requires 546.3556).

2,6-Bis(3-pyrrolidin-1-ylpropionamido)-9-(3-aminophenylamino)acridine (29). 2,6-Bisamido-9-chloroacridine **5** (500 mg, 1.0 mmol) was treated with 1,3-phenylenediamine (0.32 g) according to the general procedure to give the desired product **29** (110 mg, 19%) as an orange solid. ^{1}H NMR ($CDCl_3$): δ 1.89−1.93 (8 H, m, $N(CH_2CH_2)_2$), 2.57−2.64 (4 H, m, $COCH_2CH_2N$), 2.73−2.79 (8 H, m, $N(CH_2CH_2)_2$), 2.90−2.94 (4 H, m, $COCH_2CH_2N$), 6.13 (1 H, s, H-2′), 6.25−6.29 (2 H, m, H-4′, 6′), 6.96−7.02 (1 H, t, J = 7.9 Hz, H-5′), 7.52−7.62 (1 H, m, H-3, 5 or 4, 8), 7.65−7.66 (1 H, m, H-3, 5 or 4, 8), 7.87−791 (1 H, m, H-3, 5 or 4, 8), 7.96−8.00 (1 H, m, H-3, 5 or 4, 8), 8.11−8.12 (1 H, m, H-1/5), 839−8.40 (1 H, m, H-1/5), 11.37 (1 H, s, NHCO), 11.52 (1 H, s, NHCO). MS, *m*/*z*: 566.3232 ($C_{33}H_{40}N_7O_2$ M + H requires 566.3243).

2,6-Bis(3-pyrrolidin-1-ylpropionamido)-9-(2-aminophenylamino)acridine (30). 2,6-Bisamido-9-chloroacridine **5** (500 mg, 1.0 mmol) was treated with 1,2-phenylenediamine (0.32 g) according to the general procedure to give the desired product **30** (400 mg, 70%) as an orange solid. ^{1}H NMR ($CDCl_3$): δ 1.86−1.88 (8 H, m, $N(CH_2CH_2)_2$), 2.53−2.57 (4 H, m, $COCH_2CH_2N$), 2.60−2.69 (8 H, m, $N(CH_2CH_2)_2$), 2.82−2.87 (4 H, t, J = 5.8 Hz, $COCH_2CH_2N$), 6.55 (2 H, m, H-3′/4′/5′/6′), 6.83−6.95 (2 H, m, H-3′/4′/5′/6′), 7.11 (1 H, m), 7.59−7.71 (3 H, m), 7.95 (1 H, m), 8.25 (1 H, s), 11.13 (1 H, s, NHCO), 11.48 (1 H, s, NHCO). MS, *m*/*z*: 566.3260 ($C_{33}H_{40}N_7O_2$ M + H requires 566.3243).

2,6-Bis(3-pyrrolidin-1-ylpropionamido)-9-phenylaminoacridine (31). 2,6-Bisamido-9-chloroacridine **5** (500 mg, 1.0 mmol) was treated with aniline (0.3 mL) according to the general procedure to give the desired product **31** (240 mg, 44%) as an orange solid. ^{1}H NMR ($CDCl_3$): δ 1.86−1.92 (8 H, m, $N(CH_2CH_2)_2$), 2.55−2.62 (4 H, m, $COCH_2CH_2N$), 2.68−2.72 (8 H, m, $N(CH_2CH_2)_2$), 2.985−2.92 (4 H, m, $COCH_2CH_2N$), 6.82−6.85 (2 H, d, J = 8.6 Hz, H-2, 6), 6.90−6.96 (1 H, t, H-3), 7.18−7.24 (2 H, dd, H-3, 5), 7.55−7.66 (2 H, m, J = 9.3 and 2.2 Hz, H-3, 6), 7.84−7.88 (1 H, d, J = 9.3 Hz, H-4/7), 7.95−7.99 (1 H, d, J = 9.3 Hz, H-4/7), 8.08 (1 H, m, H-1/5), 8.37 (1 H, m, H-1/5), 11.46 (1 H, s, NHCO), 11.59 (1 H, s, NHCO). MS, *m*/*z*: 551.3114 ($C_{33}H_{39}N_6O_2$ M + H requires 551.3134).

2,6-Bis(3-pyrrolidin-1-ylpropionamido)-9-(3-(dimethylamino)propylamino)acridine (32). 2,6-Bisamido-9-chloroacridine **5** (500 mg, 1.0 mmol) was treated with *N*,*N*-dimethylpropylamine (0.4 mL) according to the general procedure to give the desired product **32** (210 mg, 38%) as a yellow solid. ^{1}H NMR ($CDCl_3$): δ 1.92−1.95 (10 H, m, $N(CH_2CH_2)_2$ and $HNCH_2CH_2CH_2N$), 2.39 (6 H, s, $N(CH_3)_2$), 2.58−2.66 (6 H, m, $COCH_2CH_2N$ and $HNCH_2CH_2CH_2N$), 2.71 (8 H, s, $N(CH_2CH_2)_2$), 2.87−2.93 (4 H, m, $COCH_2CH_2N$), 4.12−4.17 (2 H, m, $HNCH_2CH_2CH_2N$), 7.70 (1 H, m), 7.88−8.07 (4 H, m), 8.96 (1 H, m), 11.48 (1 H, s, NHCO), 11.65 (1 H, s, NHCO). MS, *m*/*z*: 560.3732 ($C_{32}H_{46}N_7O_2$ M + H requires 560.3713). Found, HCl salt: C 50.38, H 7.52, N 12.91%. Calcd (anhydrous $C_{32}H_{45}N_7O_2$·4HCl·3.0 mol of H_2O): C 50.60, H 7.30, N 12.91%.

2,6-Bis(3-pyrrolidin-1-ylpropionamido)-9-cyclohexylaminoacridine (33). 2,6-Bisamido-9-chloroacridine **5** (500 mg, 1.0 mmol) was treated with cyclohexylamine (0.35 mL) according to the general procedure to give the desired product **33** (230 mg, 41%) as a yellow solid. ^{1}H NMR ($CDCl_3$): δ 1.06−1.66 (6 H, m, $HNCH(CH_2CH_2)_2CH_2$), 1.77 (4 H, m, $HNCH(CH_2$-$CH_2)_2CH_2$), 1.95 (8 H, m, $N(CH_2CH_2)_2$), 2.59−2.66 (4 H, m, $COCH_2CH_2N$), 2.73−2.75 (8 H, m, $N(CH_2CH_2)_2$), 2.89−2.96 (4 H, m, $COCH_2CH_2N$), 3.89 (1 H, m, $HNCH(CH_2CH_2)_2CH_2$), 7.30−7.34 (1 H, m), 7.84−8.05 (4 H, m), 8.83−8.84 (1 H, m), 11.58 (1 H, s, NHCO), 11.60 (1 H, s, NHCO). MS, *m*/*z*: 557.3592 ($C_{31}H_{44}N_7O_2$ M + H requires 557.3604).

2,7-Bis(3-pyrrolidin-1-ylpropionamido)-9-(4-methoxyphenylamino)acridine (34). 2,7-Bisamido-9-chloroacridine **6** (150 mg, 0.3 mmol) was treated with *p*-anisidine (0.5 mL) according to the general procedure to give the desired product **34** (100 mg, 52%) as a bright-orange solid. Mp >320 °C. ^{1}H NMR (DMSO): δ 1.66 (8 H, m, $N(CH_2CH_2)_2$), 2.50 (12 H, m, $COCH_2CH_2N$, $N(CH_2CH_2)_2$), 2.71 (4 H, t, J = 6.8 Hz, $COCH_2CH_2N$), 3.65 (3 H, s, OCH_3), 6.62 (2 H, d, J = 8.6 Hz, H-3′,5′), 6.74 (2 H, d, J = 8.6 Hz, H-2′,6′), 7.92 (2 H, m, J = 9.3 Hz, H-3,6), 8.01 (2 H, d, J = 9.3 Hz, H-4,5), 8.33 (2 H, m, H-1,8), 10.36 (2 H, s, NHCO). MS (EI), *m*/*z*: 581.3260 ($C_{34}H_{41}N_6O_3$ M + H requires 581.3240).

2,7-Bis(3-pyrrolidin-1-ylpropionamido)-9-(2-aminophenylamino)acridine (35). 2,7-Bisamido-9-chloroacridine **6** (150 mg, 0.3 mmol) was treated with 1,2-phenylenediamine (70 mg) according to the general procedure to give the desired product **35** (90 mg, 53%) as a dark-red solid. Mp >320 °C. ^{1}H NMR ($CDCl_3$): δ 1.79 (8 H, m, $N(CH_2CH_2)_2$), 2.46 (4 H, t, J = 5.8 Hz, $COCH_2CH_2N$), 2.58 (8 H, m, $N(CH_2CH_2)_2$), 2.77 (4 H, t, J = 5.8 Hz, $COCH_2CH_2N$), 6.39 (1 H, m, H-1′), 6.48 (1 H, m, H-4′), 6.82 (2 H, m, H-1′,2′), 7.55 (2 H, dd, J = 9.3 Hz, J = 2.3 Hz, H-3,6), 7.98 (2 H, d, J = 9.3 Hz, H-4,5), 8.18 (2 H, d, J = 2.3 Hz, H-1,8), 11.26 (2 H, s, NHCO). MS, *m*/*z*: 566.3219 ($C_{33}H_{40}N_7O_2$ M + H requires 566.3243).

2,7-Bis(3-pyrrolidin-1-ylpropionamido)-9-(3-aminophenylamino)acridine (36). 2,7-Bisamido-9-chloroacridine **6** (150 mg, 0.3 mmol) was treated with 1,3-phenylenediamine (70 mg) according to the general procedure to give **36** (100 mg, 59%) as brown solid. Mp >320 °C. ^{1}H NMR ($CDCl_3$): δ 1.75 (8 H, m, $N(CH_2CH_2)_2$), 2.45 (4 H, t, J = 5.8 Hz, $COCH_2CH_2N$), 2.56 (8 H, m, $N(CH_2CH_2)_2$), 2.76 (4 H, t, J = 5.8 Hz, $COCH_2CH_2N$), 5.96 (1 H, s, H-2′), 6.04 (1 H, d, J = 7.4 Hz, H-4′), 6.12 (1 H, d, J = 8.6 Hz, H-6′), 6.85 (2 H, dd, J = 8.6 Hz, J = 5.75 Hz, H-5′), 7.69 (2 H, dd, J = 9.3 Hz, J = 2.25 Hz, H-3,6), 8.00 (2 H, d, J = 9.3 Hz, H-4,5), 8.12 (2 H, d, J = 2.3 Hz, H-1,8), 11.52 (2 H, s, NHCO). MS, *m*/*z*: 566.3249 ($C_{33}H_{40}N_7O_2$ M + H requires 566.3243).

2,7-Bis(3-pyrrolidin-1-ylpropionamido)-9-(3-dimethylaminophenylamino)acridine (37). 2,7-Bisamido-9-chloroacridine **6** (150 mg, 0.3 mmol) was treated with *N*,*N*-dimethyl-1,3-phenylenediamine (85 mg) according to the general procedure to give the desired product **37** (70 mg, 39%) as a dark-brown solid. Mp >320 °C. ^{1}H NMR ($CDCl_3$): δ 1.75 (8 H, m, $N(CH_2CH_2)_2$), 2.53 (4 H, t, J = 6.0 Hz, $COCH_2CH_2N$), 2.64 (8 H, m, $N(CH_2CH_2)_2$), 2.75 (6 H, s, $N(CH_2)_2$), 2.85 (4 H, t, J = 6.0 Hz, $COCH_2CH_2N$), 6.04 (1 H, m, J = 7.8 Hz, H-4′), 6.23 (2 H, m, H-2′,6′), 6.92 (1 H, dd, J = 7.3 Hz, J = 7.3 Hz, H-5′), 7.81 (2 H, dd, J = 9.3 Hz, J = 2.3 Hz, H-3,6), 8.02 (2 H, d, J = 9.3 Hz, H-4,5), 8.10 (2 H, d, J = 2.3 Hz, H-1,8), 11.28 (2 H, s, NHCO). MS, *m*/*z*: 594.3572 ($C_{35}H_{44}N_7O_2$ M + H requires 594.3556).

2,7-Bis(3-pyrrolidin-1-ylpropionamido)-9-(4-aminophenylamino)acridine (38). 2,7-Bisamido-9-chloroacridine **6** (150 mg, 0.3 mmol) was treated with 1,4-phenylenediamine (70 mg) according to the general procedure to give the desired product **38** (55 mg, 32%) as a dark-red solid. Mp >320 °C. ^{1}H NMR ($CDCl_3$): δ 1.79 (8 H, m, $N(CH_2CH_2)_2$), 2.45 (4 H, t, J = 6.0 Hz, $COCH_2CH_2N$), 2.57 (8 H, m, $N(CH_2CH_2)_2$), 2.76 (4 H, t, J = 6.0 Hz, $COCH_2CH_2N$), 6.48 (2H, d, J = 8.8 Hz, H-3′,5′), 6.66 (2H, d, J = 8.8 Hz, H-2′,6′), 7.60 (2 H, dd, J = 9.0 Hz, J = 2.3 Hz, H-3,6), 7.98 (2 H, d, J = 9.0 Hz, H-4,5), 8.19 (2 H, d, J = 2.3 Hz, H-1,8), 11.43 (2 H, s, NHCO). MS, *m*/*z*: 566.3225 ($C_{33}H_{40}N_7O_2$ M + H requires 566.3243).

2,7-Bis(3-pyrrolidin-1-ylpropionamido)-9-(4-(dimethylamino)phenylamino)acridine (39). 2,7-Bisamido-9-chloroacridine **6** (150 mg, 0.3 mmol) was treated with *N*,*N*-dimethyl-1,4-phenylenediamine (90 mg) according to the general procedure to give the desired product **39** (50 mg, 28%) as a dark-brown solid. Mp >320 °C. ^{1}H NMR ($CDCl_3$): δ 1.77 (8 H, m, $N(CH_2CH_2)_2$), 2.47 (4 H, t, J = 5.7 Hz, $COCH_2CH_2N$), 2.54 (8 H, m, $N(CH_2CH_2)_2$), 2.78 (4 H, t, J = 5.75 Hz, $COCH_2CH_2N$), 2.82 (6 H, s, $N(CH_2)_2$), 6.57 (2 H, d, J = 9.0 Hz, H-3′,5′), 6.77 (2 H, d, J = 9.0 Hz, H-2′,6′), 7.70 (2 H, dd, J = 9.2 Hz, J = 2.2 Hz, H-3,6), 8.01 (2 H, d, J = 9.2 Hz, H-4,5), 8.12 (2 H, d, J =

2.2 Hz, H-1,8), 11.41 (2 H, s, N*H*CO). MS, *m/z*: 594.3572 ($C_{35}H_{44}N_7O_2$ M + H requires 594.3556).

2,7-Bis(3-pyrrolidin-1-ylpropionamido)-9-phenylaminoacridine (40). 2,7-Bisamido-9-chloroacridine **6** (150 mg, 0.3 mmol) was treated with aniline (0.5 mL) according to the general procedure to give the desired product **40** (120 mg, 72%) as a bright-red solid. Mp >320 °C. ^{1}H NMR ($CDCl_3$): δ 1.74 (8 H, m, N(CH_2CH_2)$_2$), 2.46 (4 H, t, J = 5.7 Hz, COCH_2CH$_2$N), 2.55 (8 H, m, N(CH_2CH$_2$)$_2$), 2.76 (4 H, t, J = 5.7 Hz, COCH$_2$CH_2N), 6.4 (1 H, m, H-1′), 6.7 (1 H, d, J = 7.5 Hz, H-4′), 6.83 (2 H, m, H-3′,5′), 7.10 (2 H, m, H-2′,6′), 7.69 (2 H, dd, J = 9.3 Hz, J = 2.3 Hz, H-3,6), 8.04 (2 H, d, J = 9.3 Hz, H-4,5), 8.14 (2 H, d, J = 2.3 Hz, H-1,8), 11.56 (2 H, s, N*H*CO). MS, *m/z*: 551.3153 (requires $C_{33}H_{39}N_6O_2$ M + H 551.3134).

2,7-Bis(3-pyrrolidin-1-ylpropionamido)-9-(3-methoxyphenylamino)acridine (41). 2,7-Bisamido-9-chloroacridine **6** (200 mg, 0.4 mmol) was treated with *m*-anisidine (0.5 mL) according to the general procedure to give the desired product **41** (100 mg, 43%) as an orange solid. Mp >320 °C. ^{1}H NMR ($CDCl_3$): δ 1.79 (8 H, m, N(CH_2CH_2)$_2$), 2.53 (4 H, t, J = 5.3 Hz, COCH_2CH$_2$N), 2.62 (8 H, m, N(CH_2CH$_2$)$_2$), 2.83 (4 H, t, J = 5.3 Hz, COCH$_2$CH_2N), 3.64 (3 H, s, OCH_3), 6.36 (3 H, m, H-2′,4′,6′), 7.3 (1 H, m, H-5′), 7.80 (2 H, m, J = 9.3 Hz, H-3,6), 8.04 (2 H, d, J = 9.3 Hz, H-4,5), 8.16 (2 H, m, H-1,8), 11.60 (2 H, s, N*H*CO). MS, *m/z*: 581.3247 ($C_{34}H_{41}N_6O_3$ M + H requires 581.3240).

2,7-Bis(3-pyrrolidin-1-ylpropionamido)-9-(2-hydroxyphenylamino)acridine (42). 2,7-Bisamido-9-chloroacridine **6** (150 mg, 0.3 mmol) was treated with 2-aminophenol (50 mg) according to the general procedure to give the desired product **42** (100 mg, 59%) as a dark-red solid. Mp >320 °C. ^{1}H NMR ($CDCl_3$): δ 1.80 (8 H, m, N(CH_2CH_2)$_2$), 2.57 (4 H, t, J = 6 Hz, COCH_2CH$_2$N), 2.63 (8 H, m, N(CH_2CH$_2$)$_2$), 2.86 (4 H, t, J = 6.0 Hz, COCH$_2$CH_2N), 6.45 (1 H, m, H-2′), 6.59 (1 H, m, H-3′), 6.75 (1 H, m, H-4′), 6.94 (1 H, m, H-5′), 7.73 (2 H, m, J = 9.3 Hz, J = 2.25 Hz, H-3,6), 8.00 (2 H, d, J = 9.3 Hz, H-4,5), 8.16 (2 H, d, J = 2.25 Hz, H-1,8), 11.30 (2 H, s, N*H*CO). MS, *m/z*: 567.3067 ($C_{33}H_{40}N_7O_2$ M + H requires 567.3084).

2,7-Bis(3-pyrrolidin-1-ylpropionamido)-9-(2-(dimethylamino)ethylamino)acridine (43). 2,7-Bisamido-9-chloroacridine **6** (320 mg, 0.65 mmol) was treated with *N*,*N*-dimethylethylamine (0.7 mL) according to the general procedure to give the desired product **43** (110 mg, 31%) as a yellow solid. ^{1}H NMR ($CDCl_3$): δ 1.98 (8 H, m, N(CH_2CH_2)$_2$), 2.44 (6 H, s, Me), 2.62−2.72 (6 H, m, HNCH_2CH$_2$N, COCH_2CH$_2$N), 2.74−2.77 (8 H, m, N(CH_2CH$_2$)$_2$), 2.92−2.96 (4 H, m, COCH$_2$CH_2N), 3.98 (2 H, m, N(CH_2CH_2)$_2$), 7.31−7.35 (2 H, dd, J = 9.2 and 2.2 Hz, H-3,6), 8.02−8.06 (2 H, d, J = 9.2 Hz, H-4,5), 8.95 (2 H, s, H-1,8). MS, *m/z*: 546.3573, ($C_{31}H_{43}N_7O_2$ M + H requires 546.3556). Found, HCl salt: C 50.63, H 6.89, N 12.86%. Calcd (anhydrous $C_{33}H_{42}N_7O_2$·4HCl·2.7 mol of H_2O): C 50.3, H 7.14, N 13.25%.

Taq Polymerase Assay. Compounds were tested as their hydrochloride acid addition salts at 1, 10, 20, and 50 μM final concentrations in a PCR 50 μL master mix containing 10 ng of pCI-neo mammalian expression vector (Promega, Southampton, U.K.) and forward (GGAGTTCCGCGTTACATAAC) and reverse (GTCTGCTCGAAGCATTAACC) primers (200 nmol) as described previously.[17−19] The product of approximately 1 kb was visualized on a 2% w/w agarose gel following amplification (30 cycles of 94 °C for 1 min, 55 °C for 1 min, and 72 °C for 2.5 min).

Modified Telomeric Repeat Amplification Protocol (TRAP) Assay. The ability of agents to inhibit telomerase in a cell-free assay was assessed with a modified TRAP assay using extracts from exponentially growing A2780 human ovarian carcinoma cells as described previously.[17−19] The TRAP assay was performed in two steps. (a) The first is a telomerase-mediated extension of the forward primer (TS, 5′-AATCCGTCGAGCAGAGTT, Oswel Ltd., Southampton, U.K.) contained in a 40 μL reaction mix comprising TRAP buffer (20 mM Tris-HCl (pH 8.3), 68 mM KCl, 1.5 mM $MgCl_2$, 1 mM EGTA, 0.05% v/v Tween 20), 0.05 μg of bovine serum albumin, 50 μM of each deoxynucleotide triphosphate, 0.1 μg of TS primer, and 3 μCi of [α-^{32}P]-dCTP (Amersham plc, U.K.). Protein (0.04 μg) was then incubated with the reaction mix ± agent (acid addition and quaternary dimethiodide salts) at final concentrations of up to 50 μM for 20 min at 25 °C. A lysis buffer (no protein) control, heat-inactivated protein control, and 50% protein (0.02 μg) control were included in each assay. (b) While the mixture was heated at 80 °C in a PCR block of a thermal cycler (Hybaid, U.K.) for 5 min to inactivate telomerase activity, 0.1 μg of reverse CX primer (3′-AATCCCATTCCCATTCCCATTCCC-5′) and 2 units of Taq DNA polymerase ("red hot", Advanced Biotechnologies) were added. A three-step PCR was then performed: 94 °C for 30 s, 50 °C for 30 s, and 72 °C for 1 min for 31 cycles. Telomerase-extended PCR products in the presence or absence of compounds were then determined either (1) by electrophoretic separation using 8% w/w acrylamide denaturing gels and analysis by phosphorimaging or autoradiography or (2) by harvesting on Whatman filters (25 mm glass microfiber) and analysis by liquid scintillation counting.

Growth Inhibition Assay. Growth inhibition was measured in three human ovarian carcinoma cell lines (A2780, CH1, and SKOV-3) using the sulforhodamine B (SRB) assay as described previously.[30] Briefly, between 3000 and 6000 cells were seeded into the wells of 96-well microtiter plates and allowed to attach overnight. Agents (acid addition and quaternary dimethiodide salts) were dissolved at 500 μM in water and immediately added to wells in quadruplicate at final concentrations of 0.05, 0.25, 1, 5, and 25 μM. Following an incubation period of 96 h, remaining cells were fixed with ice-cold 10% w/v trichloroacetic acid (30 min) and stained with 0.4% SRB in 1% v/v acetic acid (15 min). Mean absorbance at 540 nm for each drug concentration was expressed as a percentage of the control untreated well absorbance, and IC_{50} values (concentration required to inhibit cell growth by 50%) were determined for each agent.

Binding and Kinetic Studies. Surface plasmon resonance measurements were performed using a BIAcore 2000 system with streptavidin-coated sensor chips (SA) for all experiments. This chip consists of a gold surface and streptavidin covalently immobilized on a carboxymethylated dextran layer at the surface. To prepare sensor chips for use, they were conditioned with three consecutive 1 min injections of 1 M NaCl in 50 mM NaOH followed by extensive washing with buffer. Biotinylated telomeric DNA (5′-Biot-d[$AG_3(TTAG_3)_3$]) and G-rich hairpin duplex DNA (5′-Biot-CGCGCGCG-TTTT-CGCGCGCG) in HBS buffer buffer, pH 7.4 (0.01 M HEPES, 0.15 M NaCl, 3 mM EDTA, and 0.005% (v/v) surfactant P20), were immobilized on the surface by noncovalent capture to streptavidin. Two of the flow cells were used to immobilize the DNAs, and another served as a control. Manual injection was used with 25 nM DNA and a flow rate of 2 μL/min to achieve long contact times with the surface and to control the amount of the DNA bound to the surface. The telomeric DNA folded in the presence of K^+ and formed a quadruplex during extended flow in the SPR experiments. (Folding with respect to time was checked by a series of melting/cooling experiments assessed by both CD and UV methods; after several minutes of cooling to 25 °C, the sample displayed no further change in signals with respect to time.) All procedures for binding studies were automated using repetitive cycles of sample injection and regeneration.

All ligand samples were dissolved in H_2O (1 mM) and then diluted as stock solution to 1×10^{-4} M in the running buffer, pH 7.4 (0.01 M HEPES, 0.2 M KCl, 3 M MEDTA, and 50 μL/L surfactant P20). Samples of each were prepared in filtered and degassed buffer by serial dilutions from the stock solutions. The same running buffer was used for regeneration of the surface.

Samples were injected at flow rates of 10−20 μL/min using the KINJECT command for steady-state experiments. A higher flow rate of 100 μL/min was used for the kinetic experiments to minimize mass transport effects and deliver a consistent sample plug. Double referencing subtractions were used for data analysis. The first reference subtraction eliminates the bulk refractive index change and injection noise, while the

second subtraction of a blank buffer injection eliminates any systematic changes that are characteristic of a particular cell.

Molecular Modeling Studies. All the trisubstituted acridine compounds were constructed in the computer by means of the building options in the InsightII package. A formal single positive charge was assigned to the protonated central nitrogen atom in the acridine scaffold and to each of the pyrrolidinium nitrogens in the side chains of each compound. Moreover, a net formal positive charge was assigned to the ammonium group present in the side chain linked to the acridine 9-position in compounds **7**, **9**, **10**, **18**, **19**, **28**, **32**, and **43**. All the structures were energy-minimized (2000 steps, Polak−Ribiere conjugate gradient) using the CFF force field bond lengths, bond angles, and atom types.

The X-ray crystal structure[28] of the human 22-mer telomeric sequence (PDB code: 1KF1) was used as an initial model to study the interaction between the trisubstituted acridines and telomeric DNA. The PDB coordinates file was imported into the InsightII modeling package.[39] The potassium ions in the central channel between the planes of each G-quartet were preserved, and all water molecules were deleted. The CFF force-field atom and bond types were assigned to the quadruplex, and the hydrogen atoms were automatically added. This structure was used for all the molecular modeling simulations presented in this work.

Each trisubstituted acridine was manually docked onto the 3′ G-quartet face with the three side chains pointing into each of three grooves in the DNA structure. The complex was minimized (2000 steps, Polak−Ribiere conjugate gradient) using structural restraints on the 22-mer DNA structure. Initially, it was observed that each drug could interact with the DNA through several possible orientations. Therefore, the following conformational search protocol based on high-temperature molecular dynamics was used to find the optimum energy minimum for each complex: (1) Each complex was imported into the DISCOVER_3 module of the InsightII package, and the CFF parameters were assigned for each atom and bond. (2) An atom-based summation method with 10 Å nonbonded cutoffs and a distance-dependent dielectric constant of 4.0 were used for all the subsequent calculations. (3) Each complex was subjected to 10 ps of dynamics simulation at 350 K with full constraints on the DNA. (4) The total energy variation during the high-temperature molecular dynamics was monitored, and the structures corresponding to lowest energy minima were extracted from the dynamics trajectory and minimized through a further round of 2000 steps of minimization. (5) The DOCKING module[40] of the InsightII package was used to calculate the total interaction energy E_{bind} (obtained as a sum of electrostatic and van der Waals contributions) between drug and DNA, which was used to define a ranking order (see Table 3).

The MOPAC module available in the Insight II suite with the modified neglect of differential overlap (MNDO) and PM3 parameters sets was used for full geometry optimization of the 9-anilino protonated acridine and for the calculation of partial charges on both the acridine derivative and the 3′ G-quartet array. Finally, the calculated semiempirical partial charges were used to generate representative Connolly surfaces colored by charge distribution (Figure 4).

Acknowledgment. This work was supported by program and project grants from Cancer Research UK, by grants from the Association for International Cancer Research, the European Union, and by a fellowship to S.K.B. from the Mike Mattes Trust. A significant part of this work was undertaken at the Institute of Cancer Research, where the majority of the authors were located until 2002. We are grateful to the Institute for the facilities and for a research studentship to C.M.I.

References

(1) (a) Meyne, J.; Ratliff, R. L.; Moyzis, R. K. Conservation of the Human Telomere Sequence $(TTAGGG)_n$ among Vertebrates. *Proc. Natl. Acad. Sci. U.S.A.* **1989**, *86*, 7049−7053. (b) McElligott, R.; Wellinger, R. J. The Terminal DNA Structure of Mammalian Chromosomes. *EMBO J.* **1997**, *16*, 3705−3714.

(2) Blackburn, E. H. Switching and Signalling at the Telomere. *Cell* **2001**, *106*, 661−673.

(3) Bryan, T. M.; Cech, T. R. Telomerase and Maintenance of Chromosome Ends. *Curr. Opin. Cell Biol.* **1999**, *11*, 318−324.

(4) (a) Harley, C. B.; Futcher, A. B.; Greider, C. W. Telomeres Shorten During Ageing of Human Fibroblasts. *Nature* **1990**, *345*, 458−460. (b) Allsopp, R. C.; Harley, C. B. Evidence for a Critical Telomere Length in Senescent Human Fibroblasts. *Exp. Cell Res.* **1995**, *219*, 130−136.

(5) (a) Kim, N. W.; Piatyszek, M. A.; Prowse, K. R.; Harley, C. B.; West, M. D.; Ho, P. L. C.; Coviello, G. M.; Wright, W. E.; Weinrich, R. L.; Shay, J. W. Specific Association of Human Telomerase Activity with Immortal Cells and Cancer. *Science* **1994**, *266*, 2011−2015. (b) Counter, C. M.; Hirte, H. W.; Bacchetti, S.; Harley, C. B. Telomerase Activity in Human Ovarian Carcinoma. *Proc. Natl. Acad. Sci. U.S.A.* **1994**, *91*, 2900−2904. (c) Tang, R.; Cheng, A.-J.; Wang, J.-Y.; Wang, T.-C. V. Close Correlation between Telomerase Expression and Adenomatous Polyp Progression in Multistep Colorectal Carcinogenesis. *Cancer Res.* **1998**, *58*, 4052−4054. (d) Hoos, A.; Hepp, H. H.; Kaul, S.; Ahlert, T.; Bastert, G.; Wallwiener, D. Telomerase Activity Correlates with Tumor Aggressiveness and Reflects Therapy Effect in Breast Cancer. *Int. J. Cancer* **1998**, *79*, 8−12. (e) Sano, T.; Asai, A.; Fujimaki, T.; Kirino, T. Telomerase Activity in 144 Brain Tumours. *Br. J. Cancer* **1998**, *77*, 1633−1637. (f) Tomoda, R.; Seto, M.; Tsumuki, H.; Iida, K.; Yamazaki, T.; Sonoda, J.; Matsumine, A.; Uchida, A. Telomerase Activity and Human Telomerase Reverse Transcriptase mRNA Expression Are Correlated with Clinical Aggressiveness in Soft Tissue Tumours. *Cancer* **2002**, *95*, 1127−1133.

(6) (a) Greider, C. W.; Blackburn, E. H. Identification of a Specific Telomere Terminal Transferase Activity in Tetrahymena Extracts. *Cell* **1985**, *43*, 405−413. (b) Meyerson, M.; Counter, C. M.; Eaton, E. N.; Ellisen, L. W.; Steiner, P.; Caddle, S. D.; Ziaugra, L.; Beijersbergen, R. L.; Davidoff, M. J.; Liu, Q.; Bacchetti, S.; Haber, D. A.; Weinberg, R. A. hEST2, the Putative Human Telomerase Catalytic Subunit Gene, Is Up-regulated in Tumor Cells and During Immortalization. *Cell* **1997**, *90*, 785−795. (c) Nakamura, T. M.; Morin, G. B.; Chapman, K. B.; Weinrich, S. L.; Andrews, W. H.; Lingner, J.; Harley, C. B.; Cech, T. R. Telomerase Catalytic Subunit Homologs from Fission Yeast and Human. *Science* **1997**, *277*, 955−959.

(7) Counter, C. M.; Hahn, W. C.; Wei, W.; Caddle, S. D.; Beijersbergen, R. L.; Lansdorp, P. M.; Sedivy, J. M.; Weinberg, R. A. Dissociation among in Vitro Telomerase Activity, Telomere Maintenance and Cellular Immortalization. *Proc. Natl. Acad. Sci. U.S.A.* **1998**, *95*, 14723−14728.

(8) (a) Bryan, T. M.; Englezou, A.; Dalla-Pozza, L.; Dunham, M. A.; Reddel, R. R. Evidence for an Alternative Mechanism for Maintaining Telomere Length in Human Tumors and Tumor-Derived Cell Lines. *Nat. Med.* **1997**, *3*, 1271−1274. (b) Dunham, M. A.; Neumann, A. A.; Fasching, C. L.; Reddel, R. R. Telomere Maintenance by Recombination in Human Cells. *Nat. Genet.* **2000**, *26*, 447−450.

(9) (a) Hahn, W. C.; Stewart, S. A.; Brooks, M. W.; York, S. G.; Eaton, E.; Kurachi, A.; Beijersbergen, R. L.; Knoll, J. H. M.; Meyerson, M.; Weinberg, R. A. Inhibition of Telomerase Limits the Growth of Human Cancer Cells. *Nat. Med.* **1999**, *10*, 1164−1170. (b) Zhang, L.; Mar, V.; Zhou, W.; Harrington, L.; Robinson, M. O. Telomere Shortening and Apoptosis in Telomerase-Inhibited Human Tumor Cells. *Genes Dev.* **1999**, *13*, 2388−2399.

(10) (a) Herbert, B. S.; Pitts, A. E.; Baker, S. I.; Hamilton, S. E.; Wright, W. E.; Shay, J. W.; Corey, D. R. Inhibition of Human Telomerase in Immortal Human Cells Leads to Progressive Telomere Shortening and Cell Death. *Proc. Natl. Acad. Sci. U.S.A.* **1999**, *96*, 14276−14281. (b) Corey, D. R. Telomerase Inhibition, Oligonucleotides and Clinical Trials. *Oncogene* **2002**, *21*, 631−637.

(11) (a) Damm, K.; Hemmann, U.; Garin-Chesa, P.; Hauel,N.; Kauffmann, I.; Priepke, H.; Niestroj, C.; Daiber, C.; Enenkel, B.; Guilliard, B.; Lauritsch, I.; Muller, E.; Pascolo, E.; Sauter, G.; Pantic, M.; Martens, U. M.; Wenz, C.; Lingner, J.; Kraut, N.; Rettig, W. J.; Schnapp, A. A Highly Selective Telomerase Inhibitor Limiting Human Cancer Cell Proliferation. *EMBO J.* **2001**, *20*, 6958−6968. (b) Pascolo, E.; Wenz, C.; Lingner, J.; Hauel, N.; Priepke, H.; Kauffmann, I.; Garin-Chesa, P.; Rettig, W. J.; Damm, K.; Schnapp, A. Mechanism of Human Telomerase Inhibition by BIBR1532, a Synthetic, Non-nucleosidic Drug Candidate. *J. Biol. Chem.* **2002**, *277*, 15566−15572.

(12) (a) White, L. K.; Wright, W. E.; Shay, J. W. Telomerase Inhibitors. *Trends Biotechnol.* **2001**, *19*, 114−120. (b) Mergny, J.-L.; Riou, J.-F.; Maillet, P.; Teulade-Fichou, M.-P.; Gilson, E.

Natural and Pharmacological Regulation of Telomerase. *Nucleic Acids Res.* **2002**, *30*, 839−865. (c) Neidle, S.; Parkinson, G. N. Telomere Maintenance as a Target for Anticancer Drug Discovery. *Nat. Rev. Drug Discovery* **2002**, *1*, 383−393. (d) Rezler, E. M.; Rearss, D. J.; Hurley, L. H. Telomeres and Telomerases as Drug Targets. *Curr. Opin. Pharmacol.* **2002**, *2*, 415−423. (e) Shay, J. W.; Wright, W. E. Telomerase: A Target for Cancer Therapeutics. *Cancer Cell* **2002**, *2*, 257−265.

(13) (a) Mergny, J.-L.; Hélène, C. G-Quadruplex DNA: A Target for Drug Design. *Nat. Med.* **1998**, *4*, 1366−1367. (b) Han, H.; Hurley, L. H. G-Quadruplex DNA: A Potential Target for Anti-cancer Drug Design. *Trends Pharmacol. Sci.* **2000**, *21*, 136−142. (c) Kerwin, S. M. G-Quadruplex DNA as a Target for Drug Design. *Curr. Pharm. Des.* **2000**, *6*, 441−478. (d) Haider, S. M.; Parkinson, G. N.; Read, M. A.; Neidle, S. Design and Analysis of G4 Recognition Compounds. In *DNA and RNA Binders*; Bailly, C., Wilson, W. D., Eds.; John Wiley: Weinheim, Germany, 2002; pp 337−359.

(14) Wright, W. E.; Tesmer, V. M.; Huffman, K. E.; Levene, S. D.; Shay, J. W. Normal Human Chromosomes Have Long G-Rich Telomeric Overhangs at One End. *Genes Dev.* **1997**, *11*, 2801−2809.

(15) (a) Williamson, J. R. G-Quartet Structures in Telomeric DNA. *Annu. Rev. Biophys. Biomol. Struct.* **1994**, *23*, 703−730. (b) Simonsson, T. G-Quadruplex DNA structures−Variations on a Theme. *Biol. Chem.* **2001**, *382*, 621−628.

(16) Zahler, A. M.; Williamson, J. R.; Cech, T. R.; Prescott, D. M. Inhibition of Telomerase by G-Quartet DNA Structures. *Nature* **1991**, *350*, 718−720.

(17) (a) Sun, D.; Thompson, B.; Cathers, B. E.; Salazar, M.; Kerwin, S. M.; Trent, J. O.; Jenkins, T. C.; Neidle, S.; Hurley, L. H. Inhibition of Human Telomerase by a G-Quadruplex-Interactive Compound. *J. Med. Chem.* **1997**, *40*, 2113−2116. (b) Perry, P. J.; Gowan, S. M.; Reszka, A. P.; Polucci, P.; Jenkins, T. C.; Kelland, L. R.; Neidle, S. 1,4- and 2,6-Di-substituted Amidoanthracene-9,10-dione Derivatives as Inhibitors of Human Telomerase. *J. Med. Chem.* **1998**, *41*, 3253−3260. (c) Perry, P. J.; Reszka, A. P.; Wood, A. A.; Read, M. A.; Gowan, S. M.; Dosanjh, H. S.; Trent, J. O.; Jenkins, T. C.; Kelland, L. R.; Neidle, S. Human Telomerase Inhibition by Regioisomeric Di-substituted Amidoanthracene-9,10-diones. *J. Med. Chem.* **1998**, *41*, 4873−4884.

(18) Perry, P. J.; Read, M. A.; Davies, R. T.; Gowan, S. M.; Reszka, A. P.; Wood, A. A.; Kelland, L. R.; Neidle, S. 2,7-Di-substituted Amidofluorenone Derivatives as Inhibitors of Human Telomerase. *J. Med. Chem.* **1999**, *42*, 2679−2684.

(19) (a) Harrison, R. J.; Gowan, S. M.; Kelland, L. R.; Neidle, S. Human Telomerase Inhibition by Substituted Acridine Derivatives, *Bioorg. Med. Chem. Lett.* **1999**, *9*, 2463−2468. (b) Read, M. A.; Wood, A. A.; Harrison, J. R.; Gowan, S. M.; Kelland, L. R.; Dosanjh, H. S.; Neidle, S. Molecular Modelling Studies on G-Quadruplex Complexes of Telomerase Inhibitors: Structure−Activity Relationships. *J. Med. Chem.* **1999**, *42*, 4538−4546.

(20) (a) Wheelhouse, R.; Sun, D.; Han, H.; Han, F. X.; Hurley, L. H. Cationic Porphyrins as Telomerase Inhibitors: The Interaction of Tetra-(*N*-methyl-4-pyridyl)porphine with Quadruplex DNA. *J. Am. Chem. Soc.* **1998**, *120*, 3261−3262. (b) Han, F. X.; Wheelhouse, R. T.; Hurley, L. H. Interactions of TMPyP4 and TMPyP2 with Quadruplex DNA. Structural Basis for the Differential Effects on Telomerase Inhibition. *J. Am. Chem. Soc.* **1999**, *121*, 3561−3570. (c) Shi, D. F.; Wheelhouse, R. T.; Sun, D.; Hurley, L. H. Quadruplex-Interactive Agents as Telomerase Inhibitors: Synthesis of Porphyrins and Structure−Activity Relationships for the Inhibition of Telomerase. *J. Med. Chem.* **2001**, *44*, 4509−4523.

(21) (a) Federoff, O. V.; Salazar, M.; Han, H.; Chemeris, V. V.; Kerwin, S. M.; Hurley, L. H. NMR-Based Model of a Telomerase-Inhibiting Compound Bound to G-Quadruplex DNA. *Biochemistry* **1998**, *37*, 12367−12374. (b) Heald, R. A.; Modi, C.; Cookson, J. C.; Hutchinson, I.; Laughton, C. A.; Gowan, S. M.; Kelland, L. R.; Stevens, M. F. G. Antitumor polycyclic acridines. 8. Synthesis and Telomerase-Inhibitory Activity of Methylated Pentacyclic Acridinium Salts. *J. Med. Chem.* **2002**, *45*, 590−597.

(22) (a) Mergny, J.-L.; Lacroix, L.; Teulade-Fichou, M.-P.; Hounsou, C.; Guittal, L.; Hoarau, M.; Arimondo, P. B.; Vigneron, J.-P.; Lehn, J.-M.; Riou, J.-F.; Garestier, T.; Hélène, C. Telomerase Inhibitors Based on Quadruplex Ligands Selected by a Fluorescence Assay. *Proc. Natl. Acad. Sci. U.S.A.* **2001**, *98*, 3062−3067. (b) Riou, J.-F.; Guittat, L.; Mailliet, P.; Laoui, A.; Renou, E.; Petitgenet, O.; Mégnin-Chanet, F.; Hélène, C.; Mergny, J.-L. Cell Senescence and Telomere Shortening Induced by a New Series of Specific G-Quadruplex DNA Ligands. *Proc. Natl. Acad. Sci. U.S.A.* **2002**, *99*, 2672−2677.

(23) (a) Caprio, V.; Guyen, B.; Opoku-Boahen, Y.; Mann, J.; Gowan, S. M.; Kelland, L. M.; Read, M. A.; Neidle, S. A Novel Inhibitor of Human Telomerase Derived from 10*H*-Indolo[3,2-*b*]quinoline. *Bioorg. Med. Chem. Lett.* **2000**, *10*, 2063−2066. (b) Alberti, P.; Schmitt, P.; Nguyen, C.-H.; Rivalle, C.; Hoarau, M.; Grierson, D. S.; Mergny, J.-L. Benzoindoloquinolines Interact with DNA Tetraplexes and Inhibit Telomerase. *Bioorg. Med. Chem. Lett.* **2002**, *12*, 1071−1074.

(24) Shin-ya, K.; Wierzba, K.; Matsuo, K.; Ohtani, T.; Yamada, Y.; Furihata, K.; Hayakawa, Y.; Seto, H. Telomestatin, a Novel Telomerase Inhibitor from Streptomyces anulatus. *J. Am. Chem. Soc.* **2001**, *123*, 1262−1263.

(25) Kim, M. Y.; Vankayalapati, H.; Shin-ya, K.; Wierzba, K.; Hurley, L. H. Telomestatin, a Potent Telomerase Inhibitor That Interacts Quite Specifically with the Human Telomeric Intramolecular G-Quadruplex. *J. Am. Chem. Soc.* **2002**, *124*, 2098−2099.

(26) Denny, W. A.; Cain, B. F.; Atwell, G. J.; Hansch, C.; Panthananickal, A.; Leo, A. Potential Antitumor agents. 36. Quantitative Relationships between Experimental Antitumor Activity, Toxicity, and Structure for the General Class of 9-Anilinoacridine Antitumor Agents. *J. Med. Chem.* **1982**, *25*, 276−315.

(27) Read, M. A.; Harrison, R. J.; Romagnoli, B.; Tanious, F. A.; Gowan, S. H.; Reszka, A. P.; Wilson, W. D.; Kelland, L. R.; Neidle, S. Structure-based design of selective and potent G quadruplex-mediated telomerase inhibitors. *Proc. Natl. Acad. Sci. U.S.A.* **2001**, *98*, 4844−4849.

(28) Gowan, S. M.; Harrison, J. R.; Patterson, L.; Valenti, M.; Read, M. A.; Neidle, S.; Kelland, L. R. A G-quadruplex-interactive potent small molecule inhibitor of telomerase exhibiting in vitro and in vivo antitumor activity. *Mol. Pharmacol.* **2002**, *61*, 1154−1162.

(29) Parkinson, G. N.; Lee, M. H. P.; Neidle, S. Crystal Structure of Parallel Quadruplexes from Human Telomeric DNA. *Nature* **2002**, *417*, 876−880.

(30) Wang, Y.; Patel, D. J. Solution Structure of the Human Telomeric Repeat d[$AG_3(T_2AG_3)_3$] G-Tetraplex. *Structure* **1993**, *1*, 263−282.

(31) Kelland, L. R.; Abel, G.; McKeage, M. J.; Jones, M.; Goddard, P. M.; Valenti, M.; Murrer, B. A.; Harrap, K. R. Preclinical Antitumor Evaluation of Bis-acetato-amine-dichloro-cyclohexylamine Platinum(IV): An Orally Active Platinum Drug. *Cancer Res.* **1993**, *53*, 2581−2586.

(32) Gowan, S. M.; Heald, R.; Stevens, M. F. G.; Kelland, L. R. Potent Inhibition of Telomerase by Small-Molecule Pentacyclic Acridines Capable of Interacting with G-Quadruplexes. *Mol. Pharmacol.* **2001**, *60*, 981−988.

(33) Li, G.-Z.; Eller, M. S.; Firoozabadi, R.; Gilchrest, B. A. Evidence That Exposure of the Telomere 3′ Overhang Sequence Induces Senescence. *Proc. Natl. Acad. Sci. U.S.A.* **2003**, *100*, 527−531.

(34) Hemann, M. T.; Strong, M. A.; Hao, L. Y.; Greider, C. W. The Shortest Telomere, Not Average Telomere Length, Is Critical for Cell Viability and Chromosome Stability. *Cell* **2001**, *107*, 67−77.

(35) Chang, S.; Khoo, C. M.; Naylor, M. L.; Maser, R. S.; DePinho, R. A. Telomere-Based Crisis: Functional Differences between Telomerase Activation and ALT in Tumor Progression. *Genes Dev.* **2003**, *17*, 88−100.

(36) Gavathiotis, E.; Heald, R. A.; Stevens, F. G.; Searle, M. S. Recognition and Stabilization of Quadruplex DNA by a Potent New Telomerase Inhibitor: NMR Studies of the 2:1 Complex of a Pentacyclic Methylacridinium Cation with d(TTAGGGT)4. *Angew. Chem., Int. Ed.* **2001**, *40*, 4749−4751.

(37) Haider, S. M.; Parkinson, G. N.; Neidle, S. Structure of a G-Quadruplex−Ligand Complex. *J. Mol. Biol.* **2003**, *326*, 117−125.

(38) Clark, G. R.; Pytel, P. D.; Squire, C. J.; Neidle, S. Structure of the first parallel DNA quadruplex−drug complex**.** *J. Am. Chem. Soc.* **2003**, *125*, 4066−4067.

(39) *INSIGHTII Modelling Environment*; Molecular Simulations Inc.: San Diego, CA, 1999.

(40) Luty, B. A.; Wasserman, Z. R.; Stouten, P. F. W.; Hodge, C. N.; Zacharias, M.; McCammon, J. A. A Molecular Mechanics/Grid Method for Evaluation of Ligand−Receptor Interactions. *J. Comput. Chem.* **1995**, *16*, 454−464.

JM0308693